ANALYSIS OF OPTOELECTRONICS MATERIALS

A MASTER'S THESIS

in

Electrical and Electronics Engineering

Atilim University

by

AYOOB YOUSIF AHMED ALQURQASH

May 2017

ANALYSIS OF OPTOELECTRONICS MATERIALS

A THESIS SUBMITTED TO

THE GRADUATE SCHOOL OF NATURAL AND APPLIED SCIENCES

OF

ATILIM UNIVERSITY

BY

AYOOB YOUSIF AHMED ALQURQASH

IN PARTIAL FULFILLMENT OF THE REQUIREMENTS FOR THE DEGREE OF

MASTER OF SCIENCE

IN

THE DEPARTMENT OF ELECTRICAL AND ELECTRONICS ENGINEERING

May 2017

Approval of the Graduate School of Natural and Applied Sciences, Atılım University.

_____

Prof. Dr. K. İbrahim AKMAN

Director

I certify that this thesis satisfies all the requirements as a thesis for the degree of Master of Science.

_____

Assoc. Prof. Dr. Kemal Efe Eseller

Head of Department

This is to certify that we have read the thesis "ANALYSIS OF OPTOELECTRONICS MATERIALS" submitted by "AYOOB YOUSIF AHMED ALQURQASH" and that in our opinion, it is fully adequate, in scope and quality, as a thesis for the degree of Master of Science.

_____

Assoc. Prof. Dr. Kemal Efe Eseller

Supervisor

Examining Committee Members

Assoc.Prof.Dr. Abdullah Ceylan _____

Assoc. Prof. Dr. Kemal Efe Eseller _____

Assoc.Prof.Dr. Reşat Özgür Doruk _____

Date: (22-May-2017)

I declare and guarantee that all data, knowledge and information in this document has been obtained, processed and presented in accordance with academic rules and ethical conduct. Based on these rules and conduct, I have fully cited and referenced all material and results that are not original to this work.

Name, Last name: AYOOB ALQURQASH

Signature:

ABSTRACT

ANALYSIS OF OPTOELECTRONICS MATERIALS

AYOOB YOUSIF AHMED ALQURQASH

M.S., Electrical and Electronics Engineering Department

Supervisor: Assoc.Prof.Dr. Efe Eseller

May 2017, 50 pages

Optoelectronic is a section of electronics which deals with emitting and detecting of light such as LEDs, solar cells, transistors, photodetectors. These devices synthesis of materials (Silicon, MWCNTs, SWCNTs and Graphene) has a possibility to convert the incident radiation light in to electric power or vice versa. This thesis reviews the analysis of optoelectronic materials in particular for graphene material which represents the latest episode of the explorations of the origin of materials from carbon (graphite, fullerene, CNT, MWCNTs, SWCNTs and Graphene) and highlight the exceptional properties of MWCNTs and graphene by using Raman theory. An implementation, including experiment in a laboratory on MWCNTs sample by using Raman system which inclueds spectrometer with power laser (200mW, 100mW, 50mW) and wavelength 532nm.

Keywords: Optoelectronic, MWCNTs and Graphene

ÖZ

OPTOELEKTRONİK MALZEMELERİN ANALİZİ

AYOOB YOUSIF AHMED ALQURQASH

Yüksek Lisans, Elektrik ve Elektronik Mühendisliği

Tez Yöneticisi: Doç. Dr. Efe Eseller

Mayıs 2017, 50 sayfa

Optoelektronik, ışığın yayılımı ve algılanması LED'lerin, güneş pillerinin, transistörlerin, ve fotodetektörlerin yapısı ve üretimi ile ilgili olan bir anabilim dalıdr. Cihazların sentezlenmesinde kullanılan malzemeler, (Silikon, MWCNT, SWCNT ve Grafen) radyasyon ışığını elektriğe veya tersine dönüştürme kapasitesine göre değişim göstermektedir. Bu tez, optoelektronik sistemlerde özellikle karbondan (grafit, fulleren, CNT, MWCNT, SWCNT ve Grafen) üretilen malzemelerin kökenini temsil eden grafen materyalinde bulunan karbon nanotüp malzemelerin analizini incelemekte ve MWCNT'lerin istisnai özelliklerini vurgulamaktadır. MWCNT numunesi üzerindeki deneyler, güç lazeri (200mW, 100mW, 50mW) ve dalga boyu 532nm olan Raman spektrometresi kullanılarak gerçekleştirilmiştir.

Anahtar Kelimeler: Optoelektronik, MWCNT ve Grafen

To My Parents and My Family

ACKNOWLEDGMENTS

Primarily, I thank Allah and I Praise him for giving me the ability to complete this work.

I express sincere appreciation to my supervisor Assoc. Prof. Dr. Kemal Efe Eseller for his advices, guidances, suggestions and help throughout the research.

Also, I would like to thank the staff of the department of Electrical and Electronics Engineering of Atilim University for their efforts to help the students to provide the science and knowledge.

Finally, I would like to thank my family and my friends and everyone helped me during my study.

AYOOB ALQURQASH

TABLE OF CONTENTS

LIST OF FIGURES

FIGURES

LIST OF ABBREVIATIONS

CNT - Carbon Nanotubes

MWCNTs - Multi Walled carbon Nanotubes

SWCNTs - Single Walled carbon Nanotubes

CVD - Chemical Vapor Deposition

FET - Field Effect Transistors

IC - Integrate Circuit

SCCM - Standard Cubic Centimeter per Minute

KHD - Kramers Heisenberg Dirac theory

HOPG - Highly Oriented Pyrolitic Graphite

SEM - Scanning Electron Microscope

FWHM - Full Width of Half Maximum

RBM - Radial Breathing Mode

CHAPTER ONE

INTRODUCTION

1.1 Raman Spectroscopy

Phenomenon Raman Effect found by Sir Chandrasekhar Venkata Raman (C.V. Raman) in February 1928. Which that bears his name, just rough instrumentation has been accessed. Sir Raman utilized daylight as the source and a telescope as the gatherer. He used his eyes as a sensor for this case. That such a weakness marvels as the Raman scattering were recognized was for sure wonderful. He got the Nobel Prize for physics on 11 December 1930, Bit by bit, changes in the different segments of Raman instrumentation occurred. Early research focused on the improvement of better excitation sources. Different light sources of the components were produced (e.g., bismuth, helium, zinc, lead). These ended up being unacceptable due to low light powers. The developers are included also mercury light source. An early mercury light source which had been utilized for different purposes as a part of 1914 by Kerschbaum was created [1].

In the 1930s mercury light source convenient for Raman utilization were designed. Hibben improvements has been achieved a mercury burner in1939 [1], and in 1942 Spedding and Stamm tried to find a cooled type [1]. An advance was made by Rank and McCartney in 1948, who concentrated on mercury burners and their experiences [1].

Hilger Co. Managed to find a mercury trigger source framework for the Raman instrument, which comprised of four light source enclosed the Raman tube.

Welsh et al. Presented a mercury source early from the 1950s, which got to be familiar name Toronto Arc [1]. The light source comprised of a four-source helix of Pyrex tubing and was a change over the Hilger light source. Changes in light source were made by Ham and Walsh, who portrayed the utilization of microwave-controlled helium, sodium, mercury, and Potassium light source. Stammreich likewise check the reasonableness of utilizing argon, cesium, rubidium, and helium

light source for shaded materials [1]. His work was hard for studying the propagation of light and the discovery of his influence gave him the legitimacy to carry his name. Laser discovery in 1960 by Maiman [2] gave an impetus to the improvement of implementation Raman Spectroscopy [2]. After this discovery, the sources of Raman Spectroscopy depends on the laser.

Ultimately, the Argon-ion laser which has a wavelength start from (351.lnm to 514.5nm) and the Krypton laser from (337.4nm to 676.4 nm) becomes obtainable are easy, with the passage of time exactly in (1964) appeared another kind of laser (Nd. YAG) which has a wavelength (1,064 nm). It was utilized as a source of Raman spectroscopy [1]. After this progress which appeared on a laser, gave the feature to Raman spectroscopy to become one of the important ways to an analysis of materials [2].

Through a brief period replaced the light sources (mercury) to other sources (laser). In the meantime, also, being replaced with other modern components like photomultipliers, scanning spectrometers. In parallel with the development and the discoveries of modern electronic components the Raman spectroscopy also develops [1] [2].

1.2 Carbon Nanotubes and Graphene: Discovery and Application

The evolution of modern life demands a development in technology, this prompted researchers to race for research and discovery in the area of finding materials to help improve the performance of electronic devices and increase speed and smaller size. Where Silicon was one of the dominant material in the manufacture of small electronic compound such as transistor and electronic integrated circuits (IC) with the limited theoretical and technical background. The element carbon is available in nature, its represent the source to obtain of graphite, fullerenes, carbon nanotubes and graphene [16]. Raman spectroscopy assists in achieving progress in carbon materials studies, especially the Graphene [3]. Where it's able to give us a lot of information and details, for example, the thickness of graphene, disorder and conductivity [9]. In 1960, graphite appeared on the scene were discovered by Arthur Moore *et al* [17]. In 1985, The fullerene (C_{60}) have been discovered zero dimension by Kroto *et al* [15] who (was awarded the Nobel Prize in Chemistry in 1996) [6].

Gave impetus for scientists to proceed with research and development [16]. Since this date the number of researchers has begun to increase in this field. That researches in 1991 where was found of carbon nanotubes (CNT) one dimension by Iijima [15]. CNTs is the regularity of graphene in a single, double, multi layers and wrapped up around itself. It results from that so-called (SWCNTs, DWCNTs and MWCNTs) with unparalleled properties that acquiring them possibly valuable in a wide assortment of uses such as electronic and optoelectronic uses. This label coming from the very small size of the material where has diameter very small and measured by nanometer [34]. It played a role in the discovery of (MWNTs) where the deposition was observed on the cathode electrode during preparation fullerene. Research scientists and researchers have continued for many years until he saw the light and found (SWNTs) in 1993 [16,6]. Followed in 2004 Novoselov *et al*. It has been discovered material two-dimensional namely Graphene [15]. Two dimensional comes from the height of the layer which equals to one atom of graphite which was a hexagonal lattice form the Figures (1 & 2 & 3) illustrated.

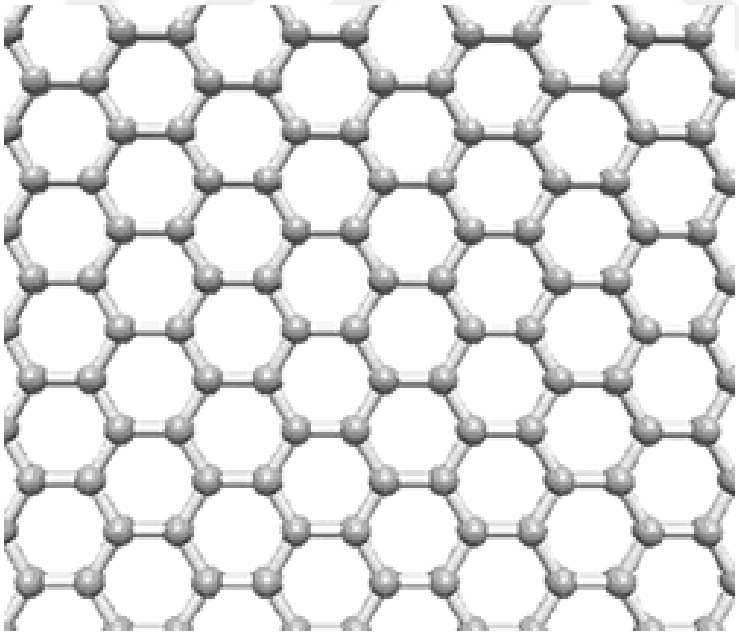

Figure (1) Carbon hexagonal lattice structure of graphene [9]

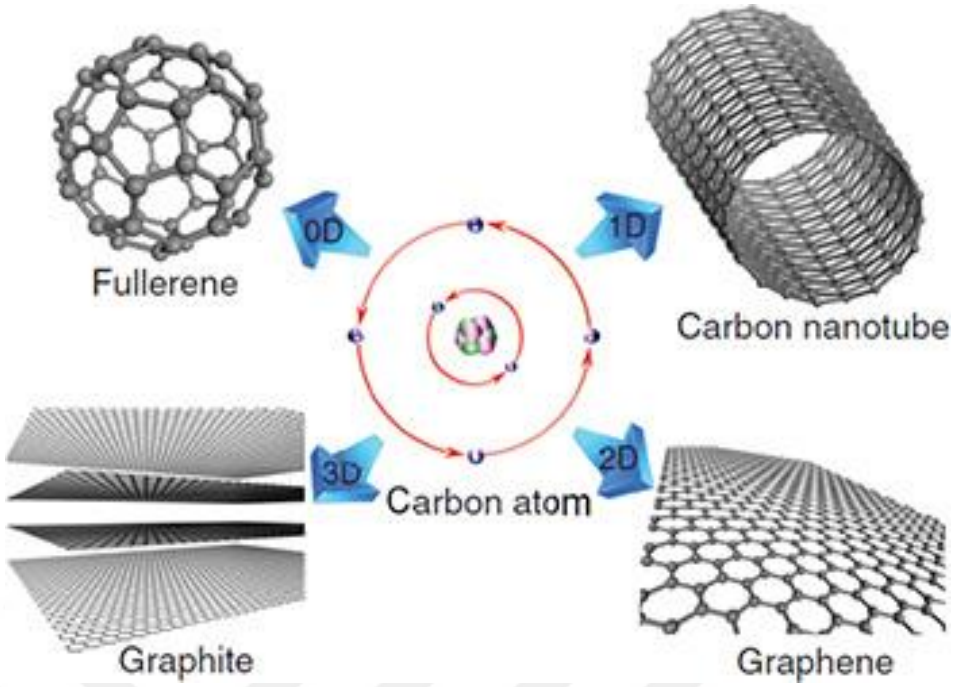

Figure (2) some substances derived from carbon atoms (0D - 3D) [35]

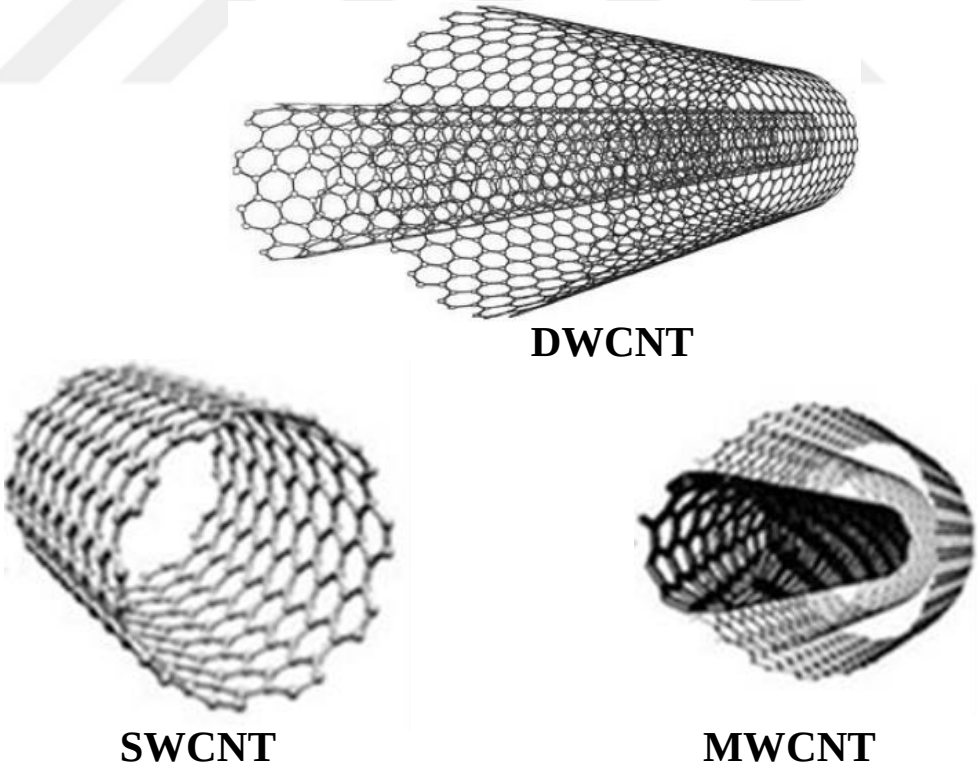

Figure (3) Single, Double and Multi-Wall Nanotubes [36]

In spite of the fact that the CNTs have one - sixth of the heaviness of steel, like graphene under stress, CNTs are two requests of size more powerful than steel. PC emulation rating of the fusion purpose of nanotubes of around 3700◦C which represents the highest degree compared to other materials, yet near the fusion degree to graphite. The diameter and in addition the structure of the CNT, play a major role in influencing the electronic conductivity of the SWCNTs. The diameter of MWCNTs ranging 2nm-50nm and the gaps between the layers inside the MWCNTs approximately 0.34nm [34,37]. There are three ways are common so far, for the production of the MWCNTs. Arc discharge, chemical vapor deposition and laser ablation way) [37]. By a wide temperature change, installation of catalyst, and different treatment parameters, the normal nanotube measurement and size allocation can be shifted. Arc discharge and laser ablation are at present the important techniques for getting little amounts of superb CNTs. In any case, both strategies have several disadvantages. Firstly, both strategies includes vaporizing the carbon sample source, therefore it has been misty how proportional up generation to the modern level utilizing these methodologies. Secondly the issue identifies with the way that vaporization techniques develop CNTs in profoundly tangled structures, blended with undesirable types of carbon or potentially metal sort. The CNTs therefore created are hard to filtered, control, and gather for creating nanotube component structures for realistic applications [37, 38].

Graphene has gotten much interest as of late in among scientists and researchers because it has distinctive properties and possibilities with the Nano electronic usages or applications [9]. Therefore, it is a quickly rising star and became a bright star between materials [8]. Previous studies have shown that the graphene doesn’t only have a high conductivity at normal temperature, but also has a lot of distinctive properties like transparency and other properties can use in manufacturing the electronic components which added to this field multi-properties for future devices [7, 9]. Add to other than the remarkable mechanical features and thermic features [16].

Graphene imposed itself as supermaterial because of its exceptional physical properties. This new sort of 2D materials which has nanostructure, it drew the attention of researchers at all disciplines. At present, graphene became the material

thinner discovered so far and the most robust material. However, it has brilliant electrical, thermal conductivity, feature optical, high stability, high flexibility, excellent porosity, and other recipes featured [15]. The stability of graphene structures comes from the ability of the carbon atom to interconnect with neighbor atoms because it has four electrons in outer orbit and formation of covalent bonds [4]. The horizontal distance between two atoms is (0.142 nm) [5]. And the vertical distance is (0.123 nm) [5, 6]. Figure (4) illustrated.

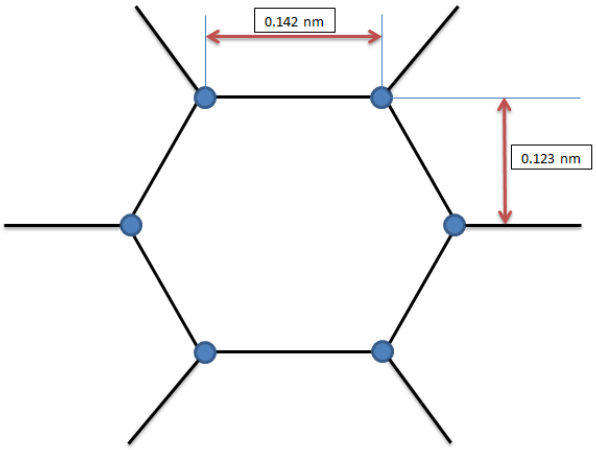

Figure (4) Digram for the distances (vertical and horizontal) between atoms graphene

In general, graphene is a new type of material with a thickness of one atom this feature gave labels two dimensional [10]. Graphene shows numerous exciting properties, for example, Hall effect at room temperature, wide range ballistic transport with just about ten times more prominent electron versatility than of Silicon, accessibility of charge bearers that carry on as massless relativistic semi molecule (Dirac fermions), and the limited of band gap comes from quantum confinement and Coulomb siege effect. These exceptional properties can be used for manufacturing excellent electronic components, for example, FET, IC, and Supercapacitors [15]. Many ways of manufacture graphene, but the most prominent are the two main, way, peeling of graphite to obtain graphene and way chemical CVD.

The first way familiar for all which known as Scotch tape, by utilizing adhesive tape to get a thin layer sample from graphite and return the operation to the sample many times to obtain a single layer with high one atom [13].

For the second way, Graphene petite accumulates by CVD method (Methane compound as carbon raw materials) on copper (Cu) substrates at the surrounding pressure. A first step, a copper foil with thickness (0.025mm) was introduced into a (CVD) oven to heat to (1050 ºC) with the existence (300 sccm Argon) and (10 sccm Hydrogen gas) in the wake of achieving 1050 ºC, the model or sample remains under 1050 ºC for half hour or more without any change in the gas influx rates. After that comes participation the Methane with the previous gasses (Argon and Hydrogen) for ten minutes. Eventually, the model was quickly cooled to normal temperature with existence Argon and Hydrogen gasses. Then bring out the product from oven [10]. The Nobel Prize in Physics at 2010 crowned two scientists is (Andre K. Geim) and (Konstantin S. Novoselov). Where they had a significant role in this achievement Graphene [12].

CHAPTER TWO

LITERATURE SURVEY

As previously mention from the stage of discovery and development of carbon material. I looked at those stages and the results of research and studies conducted in the past, but my focus will be on graphene. To be integrated search, any researcher cannot separate the specification or properties of graphene, but they are mentioning that and they focused are in part or a set of specifications. It is noted that, for example,

The researcher **Isaac Childres *et al*, CH19 [9]:** is highlighted on the properties of graphene by using Raman spectroscopy application to explain synthesis of graphene. Where they are able to study the main peaks (D, G, and 2D) in the fingerprint of the graphene and the statement of the sensitivity of its location on the Raman spectrum explains the characteristics of graphene and the state of the intensities relationship to the peaks of each peak with each other and the interest of the fund.

The researcher **Andrea C. Ferrari, 2007 [14]:** is focused on the originated of D, G and 2D peaks of graphene, the variation location, form and the relation I_{2D}/I_G to know how many graphene layers, the influence of the alloy in graphene on the form and changes in the spectrum and the graphene defect can be observed in the change of the form D peak. He relies on the Raman applications for his study.

The researcher **Ujjal Kumar Sur, 2012 [15]:** is focused on the synthesis, functions, various applications and the remarkable properties of graphene highlighted as a future material and he expects that graphene market will thrive to the highest levels.

The researcher **R. Saito *et al*, 2011 [16]:** is focused on the samples (graphene) regimes individually and relative to typical estimates of nanostructured samples. In addition to showing the capability of Raman application to detect properties of the sample (graphene) and the aspects of the convergence of the graphite. And they are emphasizing the development which obtained of the Raman theory useful to the in-depth study of the materials and state of the characterize of materials and through the spectrum to illustrate the behavior of graphene.

Eric J. Heller *et al*, 2015 [3]: adopted in their research on the theory of KHD with Raman scattering to study of graphene properties.

Qingkai Yu *et al*, 2011 [10]: is focused on the production of graphene, improve production and control to get high quality. By using the CVD method to product graphene.

A.k. Gem, 2009 [17]: is researching the progress that is happening in the research and analysis applications and tries to distinguish the future path to graphene material.

S. S. Nanda *et al*, 2016 [18]: is researching the audit the advancements and examine the future heading and different inquiries applicable to Raman spectroscopic examination of graphene and graphene-related mixes. An upgrade of the essential ideas basic the Raman spectroscopy of graphene is introduced and conclusions with respect to this matter are given. The biomedical and physical utilizations of Raman spectroscopy of graphene are evaluated. The upgrade of the Raman flags and investigations of these improvements is known as Surface improved Raman spectroscopy and Tip upgraded Raman spectroscopy. Diverse systems of the accomplishing compound upgrade of the Raman flag of the graphene surface and investigation of these improvements through Raman spectroscopy are talked about in this basic audit delineating the development in the utilization of Raman spectroscopy in a graphene survey.

The researcher **Magdalena Wojtaszek, 2009 [19]:** is highlighted in the correlation of the expectations from the model with the exploratory perceptions.

For that reason, he created graphene gadgets and measured electronic transport with and without an attractive field. In the last part, he demonstrates that in spite of the fact that the proposed model is exceptionally straightforward, it duplicates will the estimations and can fill in as an apparatus for test characterization.

Andrea C. Ferrari and Denis M. Basko, **2013 [20]:** is focused on the best in class, future headings and open inquiries in Raman spectroscopy of graphene. They portray basic physical procedures whose significance has just as of late been perceived, for example, the different sorts of reverberation at play, and the part of the quantum impedance. They have redesigned every single essential idea and documentations, and propose a wording that can portray any outcome in writing. At last, they highlight the capability of Raman spectroscopy for layered materials other than graphene.

Andreas Bablich *et al*, 2016 [21]: is highlighted on the optoelectronic gadgets in view of graphene and related two-dimensional (2D) materials. The search incorporates essential contemplations of process innovation, including exhibitions of 2D heterostructure development, and remarks on the versatility and manufacture ability of the development techniques. We then survey the capability of graphene-based straightforward leading anodes. A noteworthy part of the search depicts photodetectors in view of horizontal graphene p-n intersections and Schottky diodes. At last, the advance in vertical gadgets produced using 2D/3D heterojunctions, and additionally, each of the 2D heterostructures is examined.

F. Bonaccorso *et al*, 2010 [22]: are reviewing the Photonics and optoelectronics properties of graphene and the characteristics of the potential future application's appearance.

Frank Schwierz, 2010 [23]: surveys the properties of graphene that are significant to electronic gadgets, talk about the exchange offs among these properties and look at their impacts on the execution of graphene transistors in both rationales and radio frequency applications. He infers that the amazing versatility of graphene may not, as is regularly expected, be its most convincing component from a gadget

viewpoint. Or maybe, it might be the likelihood of making gadgets with channels that are greatly thin that will permit graphene field-impact transistors to be scaled to shorter channel lengths and higher velocities without experiencing the antagonistic short channel impacts that limit the execution of existing gadgets. Exceptional difficulties for graphene transistors incorporate opening a sizeable and all around the characterized band gap in graphene, making huge zone graphene transistors that work in the current saturation administration and creating graphene nanoribbons with all around characterized widths and clean edges.

Zhi Yang *et al*, 2012 [24]: are highlighted on the significant headway in graphene investigate: readiness, functional and additionally the specifications of graphene will be talked about. What's more, the possibility and potential uses of graphene in regions, for example, sensors, nano (electronics and composites) materials, which are also discussed. And they are talking about the techniques identified with the planning, functional, and utilizations of graphene. Over the span of the few years, it can be normal that there will be a blast of searches on the new amalgamation, functional, and also uses of graphene. Alongside the licenses and distributions, the world will witness an upset in nano-science in which a totally new manufacturing and innovation will develop, in light of graphene and the science of functional graphene.

Changsoo Park, 2015 [25]: is proposing a strategy to create (valley-polarize) electron rays utilizing two layers of graphene n-p-n intersecting. By analysis of the moving description of electrons out of the intersection with a sinuous interface within the sight of trigonal twisting, he monitored that he exists a domain collision of energies and hindrance elevations in which moved electrons are good condition polarize and aligned. To this point of perception and by performing numeral reproductions, it is exhibited that valley-subordinate electronic streams with about flawless polarization have the ability to produce. He additionally demonstrates the secession angle for the polarization current which can be under control via utilizing high and low at voltage gate. The outcomes can be utilized for building an electronic shaft splitter to deliver valley - polarize streams. He exhibited that (valley- polarize) electronic streams with about full polarize can be created in two layers of graphene

n-p-n intersecting. The conjunction with the separate boundary conditions of the energies which carry a negative sign motivate the electrons with the energies which carry a positive sign to submit to the angle which conditional to a resonant motion which is described and distributed with energy conservation. Within the sight of trigonal twisting, this empowers the moved electron streams to be very much polarized and aligned. He has demonstrated the polarize streams has the ability to exist in a different domain of energies and hindrance elevations and the location partition between the values of the highest point (peaks) estimations of the polarize streams and the ability of controller by outer gate voltage. By building an electron shaft splitter in view of the present outcomes, it can get polarize streams very much isolated in space, which might be utilized for a (valley-based) electronic gadget as well as for researching impedance impacts between valley polarize waves.

Chao Qiu *et al*, 2016 [26]: is searched and introduce detailed search with Raman application and Drude system to an investigation of variations and upgrades in a material's properties, as it moves from three-dimensional (graphite) to two dimensional (graphene). In addition to registration by Raman system, which demonstrates regardless mono layer, a dual layer, or more than that of graphene, the Raman application mapping authorized to the uniqueness of such range and an immediate imagination of the homogeneity of the material. Besides, the estimations or identify the value of IR transmittance and utilization of the Drude system, both identified with the material, conductivity of electrical, exhibit a featured increment in conductivity if reduced dimensional, from $92.1\ \Omega^{-1}\text{cm}^{-1}$ For an (HOPG) specimen to 2138 $\Omega^{-1}\text{cm}^{-1}$ For a specimen with a mono layer to a some layer of graphene. This mensuration is additionally especially suited to deciding other significant material qualities, including a significant rise in the concentration of carrier ($3.59 \times 1018\ \text{cm}^{-1}$, $14.91 \times 1018\ \text{cm}^{-1}$, $46.31 \times 1018\ \text{cm}^{-1}$) For (HOPG), the more than one layer, mono layer of graphene respectively. These last outcomes it shows the importance and dominance the transport of intralayer adds to the conductivity of the material. Such detail and data are important for improving the sensors for biomedical, where is representing the fundamental application imagined for this search.

Shaahin Amini *et al*, 2010 [27]: is exhibited another (method) or strategy for the huge range graphene development, which gave an ability to new methods of production with lower costs and high productivity. The technique depends on developing mono layer or some layer of graphene velum from a fusion stage. The procedure includes dissolution of carbon with a fused metal at a given temperature and afterward permitting the dissolution or broke up carbon to a first thermodynamic stage (nucleate) and develop on the surface of the fused metal with less a temperature. The inspected metals of the carbon dissolution included (Cu) and (Ni). For the last mentioned, the brilliance of one layer of graphene was developed effectively. The outcome of graphene layers was undergone to itemized infinitesimal and Raman spectroscopic portrayal. The de convolution of the Raman two-dimensional band was utilized to precisely decide the quantity of nuclear plans in the outcome graphene layers and get to their goodness. The outcomes demonstrate for their innovation can give mass graphite velum, some layer of graphene and additionally high productivity mono layer of graphene on the metals. Their working style can likewise be utilized for creating graphene thermic mediator materials for thermic administration applications.

Takaaki Tomai, Yuji Kawaguchi, and Itaru Honma, **2012 [28]:** They are explaining that the nano-graphene was created from sheets, carbon lattice via the method of (SCF) peeling without sour oxidation. Amid the peeling procedure, a dynamic abatement in the quantity of layers was joined via the cutting process of the basilar plane. They depend on the Raman application to recognize the nature of the specimens, declaring that the deformity thickness in the basilar plane of the nano-graphene which has the ability to lessen to not as much as that of a beginning material amid (SCF) peeling.

C. Casiraghi *et al*, 2007 [29]: they are highlighted on the powerful differences in the Raman spectrums of various mono-layer for graphene specimens acquired by micro mechanical splitting. This detects the existence of overabundance in the charges, even without deliberate doping. The concentrations of doping if increased to more than 10^{13}cm^{-2} are assessed by study the shape, deviation and domain of pulse G and the diversity of the location and the intensity I_{2D} for the pulse 2D.

Asymmetry of the pulse G show charges disproportionate on a size of under 1 μm. Add more details about their search, they demonstrate that Raman application can fingerprint contrasts between ostensibly indistinguishable specimens created similarly. They found that, the regardless presence a D pulse, manipulation via the parameters of Raman which are more normal and associated with an existence of overabundance in the charges. This is an important result, which accommodates the variety of electrical features regularly found in ostensibly indistinguishable specimens. They focused on as enough of specimens above 40 mono layer graphene, delivered by small scale division of graphite. Which have distinctive regions, ranging a limited number of ($\mu m^2 \rightarrow 450 \mu m^2$). They are working on getting enough number of the spectra over 100, by utilizing source laser (514 nm and 633nm) with resolution 2cm^{-1} with power less than 2 mW.

Katsuhisa Murakami, Takuya Kadowaki, and Jun-ichi Fujita, **2013 [30]:** Focused their search on the study of the relationship (I_D/I_G) by using Raman applications, electron stream radiation with the approximate energy of (100eV) which has the ability to occur damaged in the monolayer of graphene. The harm or damage gets to be distinctly bigger with diminishing electron stream energy. Inner stress, which occurs for graphene instigated by harm under radiation is moreover assessed in view of G pulse shifts. The dosage dependent on the inner stress was around (2.22% - 2.65×10^{-2}%) $\frac{\text{cm}^2}{\text{mC}}$ at 100eV and 500eV respectively. The stress instigated by the radiation indicated a solid reliance on electron energies.

Sebastián R. Accordino *et al*, 2015 [31]: Graphene and the materials that originate from carbon such as graphite, CNT, C60, MWNTs and SWNTs are normally viewed as hydrophobic as well as have been generally utilized as ideal models for the realization of the conduct with the proviso, nonpolar detention for water, an issue of real sympathy toward field's domain for biology science to materials styling. But, some experiential and academic bits of knowledge appear to repudiate, in any event, in part, such a photo. In this search, they provided irrefutable evidence of a flawless hydrophilic kind of graphene superficial. Their studies of the components of atoms showed that analogous graphene sheets, insert a solid the

propensity to stay completely hydrated for middling for a long period of time (notwithstanding, when the harmony state is to be sure the breakdown of the sheets), and in this way, they are minimally inclined to self-get together than the pattern hydrophobic superficial they utilized as a control that which easily guided a hydrophobic breakdown. The capability of mean drive estimations they without a doubt make obvious the dissolvent make a repulsion commitment to the self-get together of graphene superficial. Besides that, they likewise evaluate graphene hydrophilicity via a method for the figuring the density of water at two cases of pressures and water density variances. This search has not been implemented on graphene and speaks to a method both to affirm and to evaluate its flawless hydrophilic conduct. They likewise make clear the pertinence of the somewhat alluring water-carbon admixture or interactions.

M. Reininghaus *et al*, 2012 [32]: Their search was on the theme a laser incited removal procedure to manufacture ultra thin graphite wafers. By changing the fluence of the removing beam Full Spectrum Laser (FSL) irradiation, they identify features numeric for thermic vaporization thus called the non-thermic removal of graphite wafers. The existence of a non-thermic removal is an immediate outcome of the solid mismatch of the strength of cohesion in a natural casing and the direction of the plane of the material which has layers, for example, graphite. The non-thermal removal threshold of graphite is 250 $\frac{\text{mJ}}{\text{cm}^2}$ which obtained through experiments concurs completely with academic forecasts. Lastly, they saved nano-thin graphite wafers has area 50 μm^2, Raman applications were the main method to complete this work.

Matthew J. Allen *et al*, 2008 [33]: Touched in their studies the speak about, the reduced or decreased the oxide for graphite (RGO) has indicated guarantee as an adaptable, ready to replace the mechanically way for peeling samples of graphite. Albeit numerous estimations demonstrate that (RGO) has features drawing closer those of inherent graphene, where it was difficult to know to what extent graphite system is reconditioned upon decrease. Raman applications are broadly utilized for the description of mechanically peeling graphene, however, it could not be completely investigated for (RGO).

Explain their search, hydrazine (N2H2) suspensions of (RGO) are kept on smaller scale hot-platelet and analyzed over a scope of temperatures via Raman applications. The search focused the advantage of the arrangement processing.

CHAPTER THREE

BASIC CONCEPTS OF THE THEORY OF RAMAN SPECTROSCOPY

In general, the definition of spectroscopy is the investigation and survey of interaction and changes that occur in the sample due to the incident radiation. Spectroscopy is widely utilized to research the inner structure of materials, chiefly molecules of complicated organic components or inorganic components. Three of the most common types of molecular spectra, microwave (rotational) spectra, infrared (rotational-vibrational) spectra and visible (electronic band) spectra. In this study, the interested was about a visible type, where I used laser source (532nm) and I focused on the vibrational section [12, 16]. To start speaking about the theory of Raman Spectroscopy I will explain some phenomenon's, behavior, some terms, rules and laws for molecule.

Heteronuclear, a molecule consist of multi kinds of elements. But homonuclear it is consists of just a single kind of element.

3.1 The harmonic oscillator

The harmonic oscillator, it's the oscillation fixed for any system between two values. The restoring force is assumed to obey Hooke's law (if we have spring and two masses or the spring fixed from one terminal to wall and the second terminal fixed with the masses. In the case of the draw of mass and extend of the spring, when the mass becomes free the spring will presses. The restoring force equals the distance between the equilibrium case and the extent case, multiply by the constant of spring) this is simply an idea of Hook's law. The Figure (5) illustrates two balls (m1, m2) and spring.

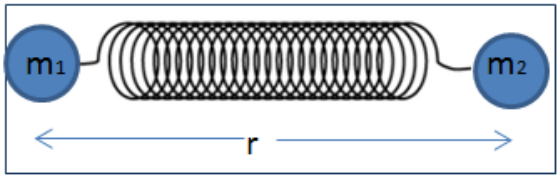

Figure (5) simple harmonic oscillator model

Restoring force = $-\frac{dP(x)}{dx} = -kx$ (3.1)

Where $P(x)$ is the potential energy, $x = (r - r_e)$ Is the displacement from the equilibrium bond length r_e , and k is the force constant. By integration of eq. (3.1) Get.

$P(x) = \frac{1}{2}kx^2$ (3.2)

For a diatomic molecule, the harmonic oscillator treated the vibrational energy levels E_v Which, given by

$E_v = hV(v + \frac{1}{2})$ (3.3)

Where vibrational quantum no. $v = 0, 1, 2, \ldots$. V: Vibrational frequency which can find it by the eq. $V = \frac{1}{2\pi}\sqrt[2]{k/\mu}$ (3.4)

Reduced mass $\mu = \frac{m1m2}{m1+m2}$ ……. (5)

It's axiomatic, the vibrational frequency V direct proportionality with k and inverse proportionality with μ.

More utilize the term vibration wavenumber symbol ω , rather than the term frequency, the eq. (3.3) Will become

$E_v = hc\omega(v + \frac{1}{2})$ (3.6)

For all diatomic molecules having two terms (rotational term values and vibrational term values) the vibrational term values will give by the eq. (3.7)

$\frac{E_v}{hc} = G(v) = \omega(v + \frac{1}{2})$ (3.7)

From eq. (3.7), if we substitute the values of $v = 0, 1, 2, 3, \ldots\ldots$ We get

$$G(0) = \frac{1}{2}\omega\,, G(1) = \frac{3}{2}\omega\,, G(2) = \frac{5}{2}\omega\,, G(3) = \frac{7}{2}\omega\,, \ldots\ldots\ldots\ldots$$

From above, we can argue the molecules impossible at $v = 0$ have not the vibrational energy because of the vibrational term equal half vibration wavenumber even at a temperature of absolute zero. In other words, the molecules have vibration energy at zero level. But the molecules have zero-point energy.

In transition case between two different levels adjacent,

Supposed $v \to v + 1$

$$\frac{\Delta E}{hc} = G(v+1) - G(v) = \left(v + 1 + \frac{1}{2}\right)\omega - (v + \frac{1}{2})\omega = \omega \qquad (3.8)$$

Obviously, we find that the distances between all the levels are equal, that's only for harmonic oscillator approximation. Figure (6) illustrated.

$$\Delta v = \pm 1$$

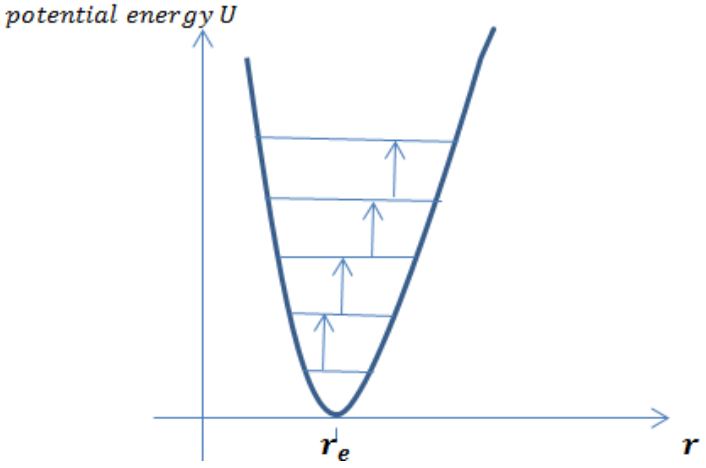

Figure (6) levels energy in harmonic oscillator case

3.2 The anharmonic oscillator

In this case, the molecule does not obey Hook's law. We will back to the values of $x = (r - r_e)$

* $(r > r_e)$ In this case the molecules dissociate and $k \to 0$ without additional change U. Consequently the curve of potential energy of anharmonic oscillator in Figure (7) we will get $U = D_e$

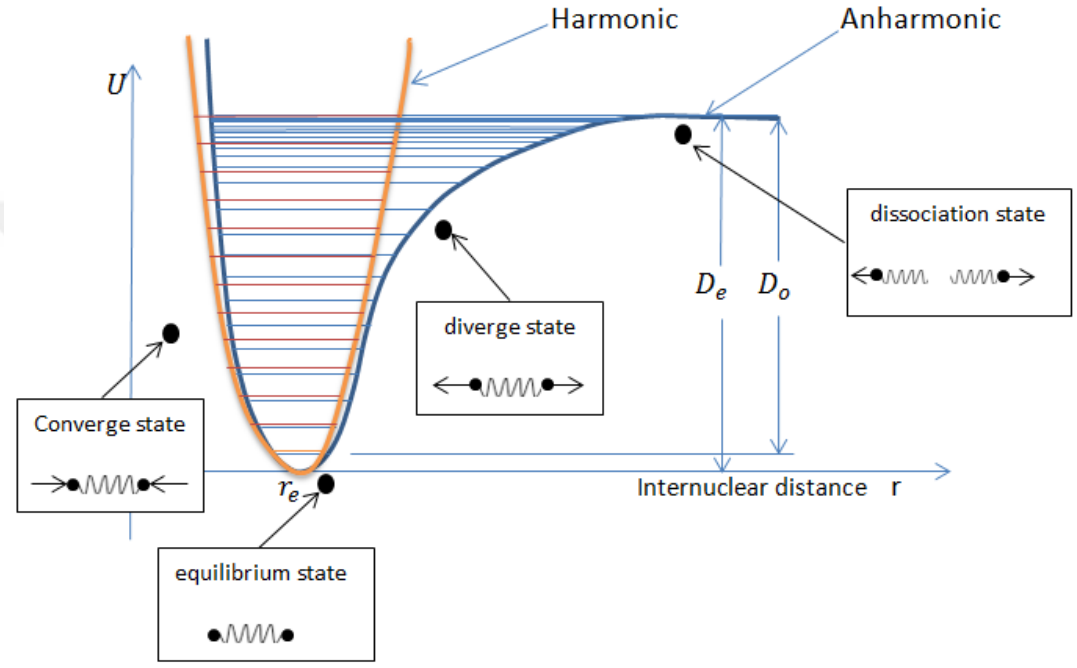

Figure (7) graphic shows the comparative in behavior between harmonic and anharmonic oscillation.

* $(r < r_e)$ In this case, similarities in charges for the two nuclei increased repulsion, the curve of a harmonic oscillator, it's more sharper compared with an anharmonic oscillator, the mechanical anharmonic very important which modifies $G\ (v)$ for eq. (3.7) as serious [12].

$$G(v) = \omega_e \left(v + \frac{1}{2}\right) - \omega_e x_e (v + \frac{1}{2})^2 + \omega_e y_e (v + \frac{1}{2})^3 + \qquad (3.9)$$

Where $\omega_e x_e$, $\omega_e y_e$ … Are anharmonic constants, the reason that the second term has a negative sign, this is due to $\omega_e x_e$ Which has a same sign with regard to the whole diatomic molecules as well the term included a negative sign, therefore it's

always positive [12]. From figure (7) we can observe the rapprochement between D_e (Which represented an accumulation of the energy levels) and the anharmonic levels. As well as we can't directly measure it, because the molecules are never at the bottom of the potential energy well the lowest energy they can possibly have is one in which they are in the $v = 0$ which is slightly above the bottom of the potential energy, so we never really measured D_e We always measure the dissociation energy D_o From the $v = 0$ level, then we have to do a little bit of math to get the formula that we can calculate the value of D_e and we can obtain the approximately of $D_e \cong \frac{\omega_e^2}{4\omega_e x_e}$

And we get $D_o = \sum_v \Delta G_{v+\frac{1}{2}}$ Where $\Delta G_{v+\frac{1}{2}} = G(v+1) - G(v)$

Presented Morse in 1929 suggested about potential energy represented by

$$U(x) = D_e[1 - e^{(-ax)}]^2 \tag{3.10}$$

By using the Schrodinger eq. With Morse eq. For case anharmonic oscillator

$$H\psi = E\psi$$

(Kinetic energy +potential Morse energy) $\psi_{vib} = E_{vib}\psi_{vib}$

$$\{-\frac{\hbar^2\partial^2}{2\mu\partial x^2} + D_e(1 - e^{-ax})^2\}\,\psi_{vib} = E_{vib}\,\psi_{vib} \tag{3.11}$$

Solving eq. (3.11) we get that the quantized obtained the vibrational energy levels. And we will reveal the distance between the energy levels adjacent it is not equal.

$$G(v) = \left(v + \frac{1}{2}\right)\omega_e - (v + \frac{1}{2})^2\omega_e x_e \tag{3.12}$$

If we substituted $v = 0, 1, 2, 3 \ldots \ldots$ We will get

$$G(0) = \frac{1}{2}\omega_e - \frac{1}{4}\omega_e x_e \quad , \quad G(1) = \frac{3}{2}\omega_e - \frac{9}{4}\omega_e x_e$$

$$G(2) = \frac{5}{2}\omega_e - \frac{25}{4}\omega_e x_e \quad , \quad G(3) = \frac{7}{2}\omega_e - \frac{49}{4}\omega_e x_e$$

Now if we calculate finding ΔG

$$\Delta G = G(1) - G(0) = \omega_e(1 - 2x_e)$$

$$\Delta G = G(2) - G(1) = \omega_e(1 - 4x_e)$$

$$\Delta G = G(3) - G(2) = \omega_e(1 - 6x_e)$$

We can see that clearly in figure (7) for the anharmonic curve.

3.3 Overtone and hot bands

The overtone occurs at second order, third order, etc. and can be getting it at the transitions between the energy levels which are not adjacent $\Delta v = +2, +3, +4$, etc., but the hot band getting it at the transitions between the energy levels, which are adjacent. Whereas the fundamental band can be seen between $(v = 0 \rightarrow v = 1)$ this is shown in figure (8), [12,13].

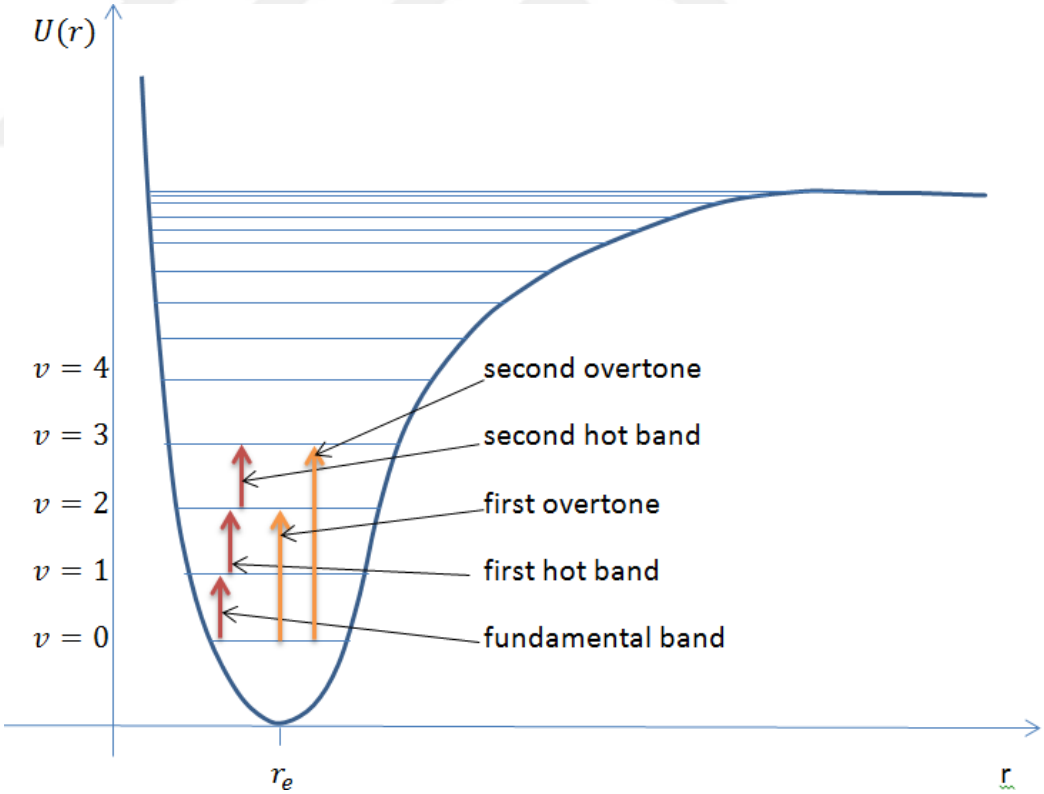

Figure (8) overtone and hot band

3.4 Vibrational and rotational levels

In Figure (9) we can observe the interference and correlation between the vibration level with rotation level.

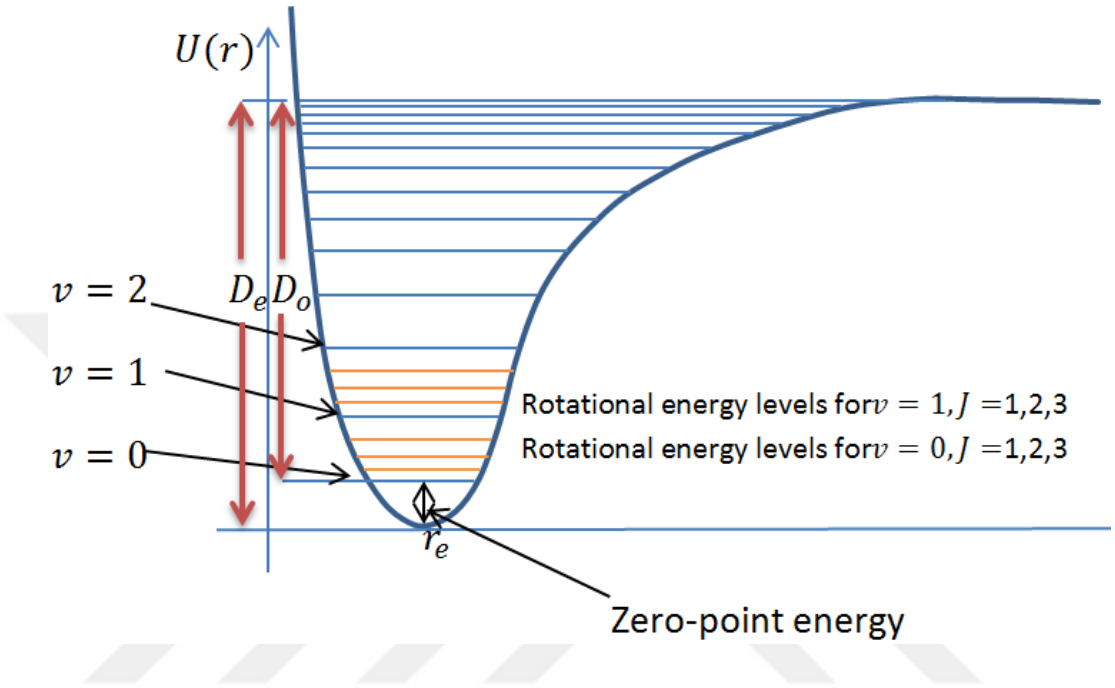

Figure (9) graphic shows the vibrational and rotational levels

In Figure (10) we make zoom in to focus on the state $v = 0, 1$ state and expand it. The zigzag illustrates the big gap in energy between the energy levels associated with $v = 0$ and those associated with $v = 1$ all the levels identified with $v = 0$ and $v = 1$ have exactly the same amount of vibrational energy $G(0) = \frac{1}{2}\omega_e - \frac{1}{4}\omega_e x_e$ And $G(1) = \frac{3}{2}\omega_e - \frac{9}{4}\omega_e x_e$ Respectively. The levels which labeled by $J = 2$ at $v = 0$ and $v = 1$ were in a pretty have the same rotational energy.

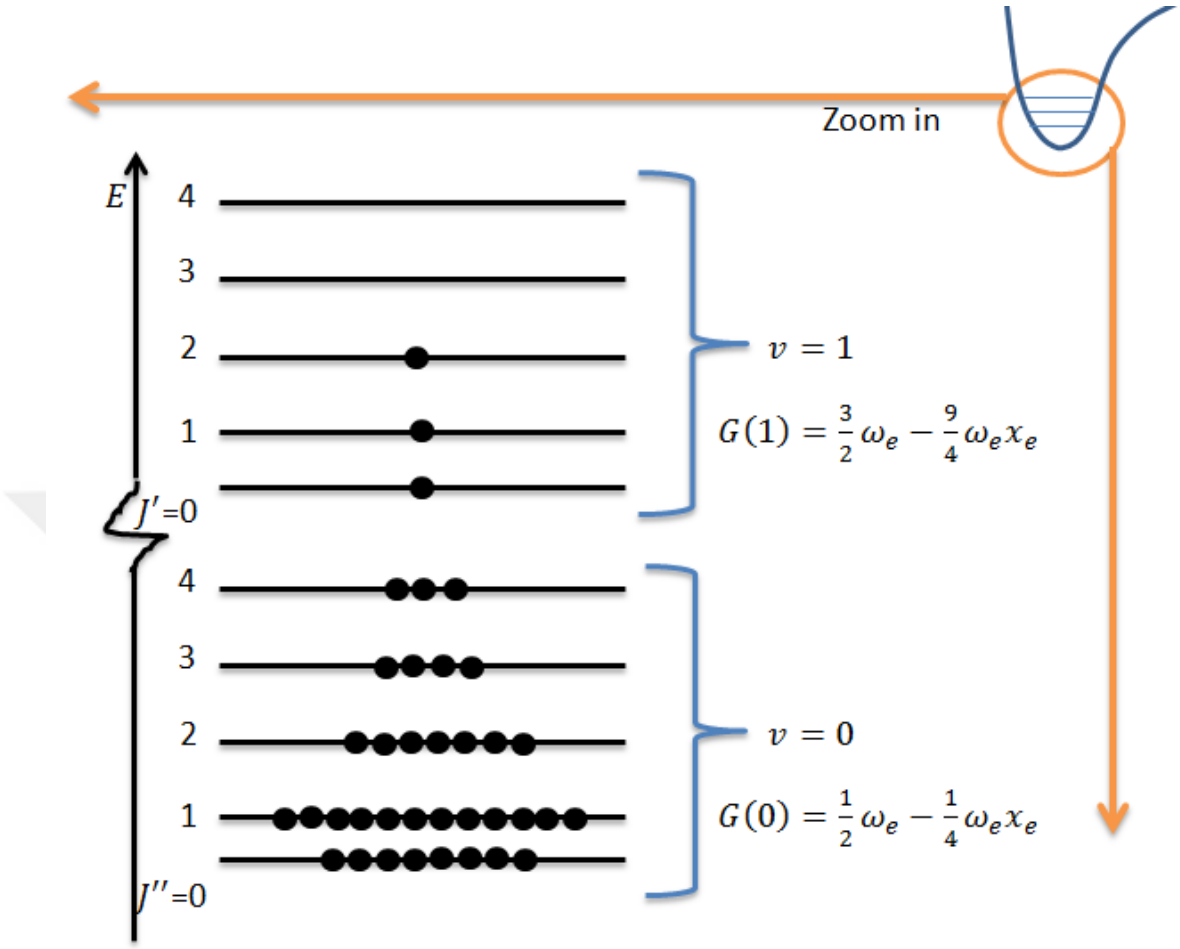

Figure (10) zooms in illustrating vibrational and rotational levels

3.5 Vibration and Rotation Spectroscopy

The transitions for molecule between the energy levels has two types of motion (vibration motion and rotational motion) with taking into consideration gas, solid or liquid phases because the vibrational transition can be sensed at all phases but the rotational transition can be sensed at gas phase. Therefore, we will take a total of two terms vibrational $G(v)$ and rotational $F_v(J)$ which represent $S(v,J)$ with omitted centrifugal distortion. The total energy $S(v,J)$ has been just a simple sum of two terms.

$$S(v,J) = G(v) + F_v(J) \tag{3.13}$$

$$= \left(v + \frac{1}{2}\right)\omega_e - (v + \frac{1}{2})^2\omega_e x_e + \ldots\ldots + B_v J(J+1) \tag{3.14}$$

Where B_v Rotational constant, J rotational quantum number

To predict the spectrum that will result from vibrational transitions we need to take into account both the selection rules that $\Delta v = \pm 1, \pm 2, \ldots..$ And $\Delta J = \pm 1$, but of course transitions for $\Delta v > \pm 1$ will exhibit far weaker spectral line intensities.

Now, will focus on the fundamental band which we will excite molecules from, $v = 0$ to $v = 1$, which will get on transitional in the $\Delta J = \pm 1$ state. And the Figure (11) illustrated.

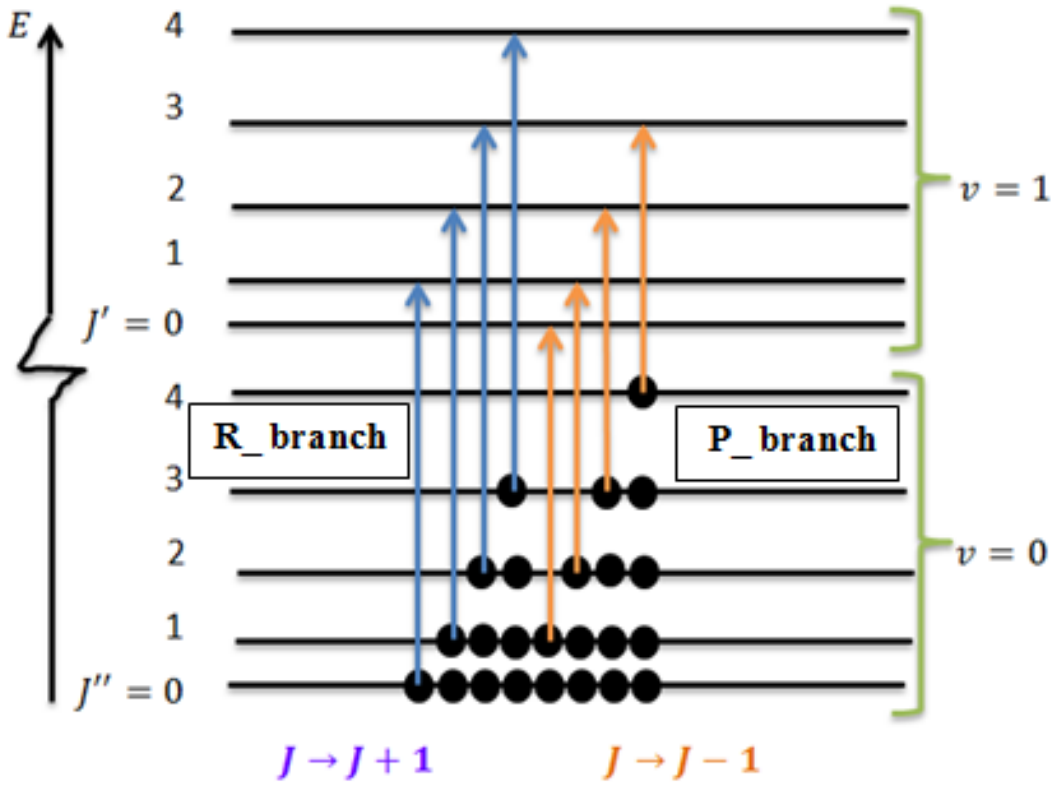

Figure (11) transition between levels

When $J \rightarrow J+1$ we identify these transitions as R – branch transition notice that all these transitions when $J \rightarrow J+1$ will be at a frequency that is larger than the fundamental frequency and the fundamental frequency can be identified in a

hypothetical transition which constant for both, and we will identify these transitions as a P – branch transition in case $J \rightarrow J-1$ and we notice the frequency, in this case is smaller than the fundamental frequency.

At the fundamental band the P – branch and R – branch we have rotational transition state between two levels, therefore we surpassed the initial state labeled (J'') And the final state is(J'), this is purely a convention. Therefore $J' = J'' - 1$ at a P – branch transition this means we can find the frequency $V_{P(J')}$ Of any line in the P – branch which represented by the difference between the total rotational and vibrational (Rovibrational) energy of the final energy level and the total Rovibrational energy of the initial energy level.

$$V_{P(J')} = G(1) + BJ'(J'+1) - G(0) - BJ''(J''+1) \tag{3.15}$$

Now we will rearrange this equation

$$V_{P(J')} = \omega_e(1-2x_e) + BJ'(J'+1) - B(J'+1)(J'+2)$$

$$= \omega_o - 2B(J'+1) \tag{3.16}$$

The same steps will apply in the case of R–branch $(J'' \rightarrow J' = J''+1)$

$$V_{R(J'')} = G(1) + BJ'(J'+1) - G(0) - BJ''(J''+1)$$

$$= \omega_e(1-2x_e) + BJ'(J''+1)(J''+2) - BJ''(J''+1)$$

$$= \omega_o + 2B(J''+1) \tag{3.17}$$

We never get a transition at exactly the fundamental frequency these two equations (3.16, 3.17) to find all the possible spectral lines in the P – branch and in the R – branch there is no other branch for diatomic. The minimum value of (J') Is zero in the P – branch and if we substitute this value in the eq. (3.16) the first line will be at $(\omega_o - 2B)$ and the minimum value of (J'') Is Zero in the R – branch as well, and substitute this value in the eq. (3.17) will get the first line in this branch will be at $(\omega_o + 2B$).

This means there's got to be a gap equal $(4B)$ between the first line in P – branch and the first line in R – branch and the middle of the gap represented the fundamental frequency (ω_O). Now it's easy to find the first line in both cases P – branch and R – branch if we know the value of gap and vice versa. And the Figure (12) illustrated.

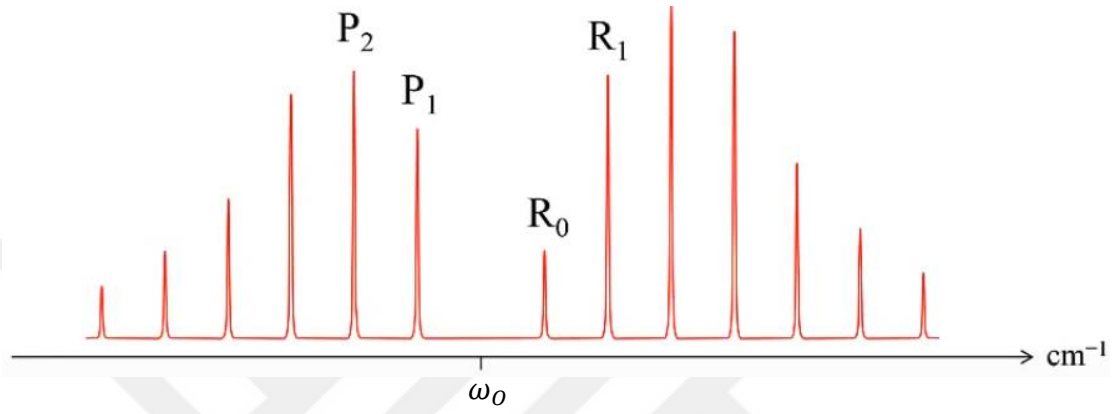

Figure (12) Rovibrational Spectrum [13]

In the diatomic molecules (homonuclear and heteronuclear) polarizability varies through the vibration motion produces the vibrational Raman Effect.

This variety can be conceived as a result of the polarizability as a shape of ellipsoids in Figure (13) converge and diverge are same the change case of bond length with vibration. Raman scattering requires that an oscillating molecular dipole is first induced prior to the inelastic scattering event this is usually accomplished with a strong electric field such as the one supplied by an intense laser. It's necessary that the electronic distribution about the molecule can be distorted by the applied electromagnetic field and that the molecular polarizability varies as a function of molecular motion (vibrational or rotational). Consider we applied electromagnetic field on a homonuclear diatomic molecule this field will affect inside the molecule.

And the resultant dipole moment, which gave by $\bar{M} = \alpha \bar{E}$ (3.18)

Where α is the polarizability which is showing the degree of separation for the electrons proportion to the nuclei. The magnitude of $\bar{E}$ Is $E = Asin2\pi c\tilde{\nu}t$ where $\tilde{\nu}$ Is wavenumber of radiation.

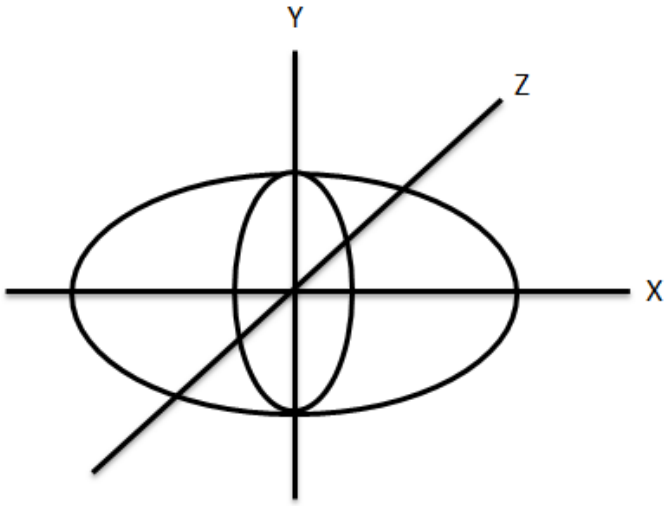

Figure (13) the polarizability as the shape of the ellipsoid [12]

By using mathematical treatments with the eq. (3.18) we get

$$M = \alpha_{o,v}Asin2\pi c\tilde{\nu}t - \frac{1}{2}\alpha_{1,v}Acos2\pi c(\tilde{\nu}+\omega)t + \frac{1}{2}\alpha_{1,v}Acos2\pi c(\tilde{\nu}-\omega)t \qquad (3.19)$$

Where $\alpha_{o,v}$ Average polarizability, $\alpha_{1,v}$ Amplitude of the change, ω vibration wavenumber.

In the eq. (3.19) the first term at right hand represents Rayleigh in this case the molecular state fixed, unchanged by interaction, the second term represents Anti-Stokes $(\tilde{\nu}+\omega)$ and the third term represents Stokes $(\tilde{\nu}-\omega)$ Raman scattering. The Figure (14) illustrated [12, 13, 14].

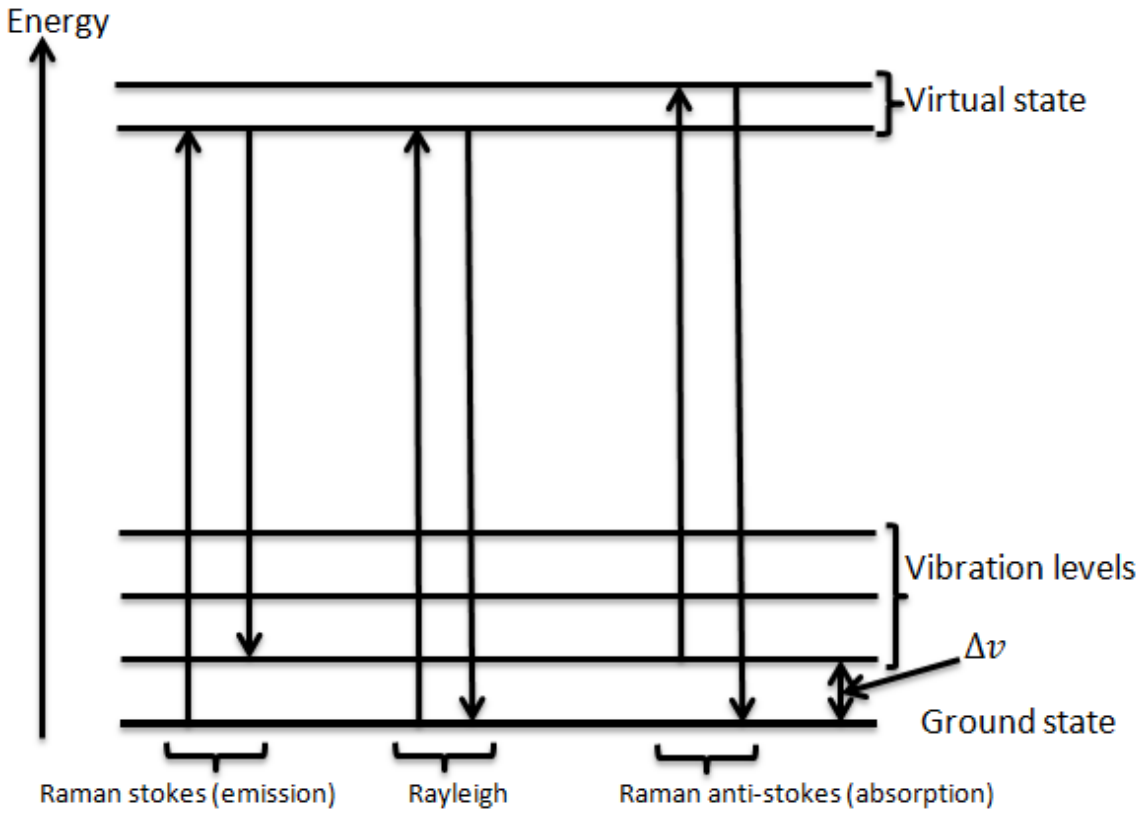

Figure (14) Vibration Raman scattering

By definition vibrational Stokes transitions is associated with vibration excitation of the molecule during the scattering process this lead to scattered lighter with a lower frequency than the incidentally concomitant with the vibrational excitation. We must also consider the $\Delta J = 0, \pm 2$ selection rules transition in which (J) changes (+2) are known as (S _ type) transitions and (Q _type) transitions where (J) does not change and (O _ type) where (J) changes (-2). The Figure (15) illustrated.

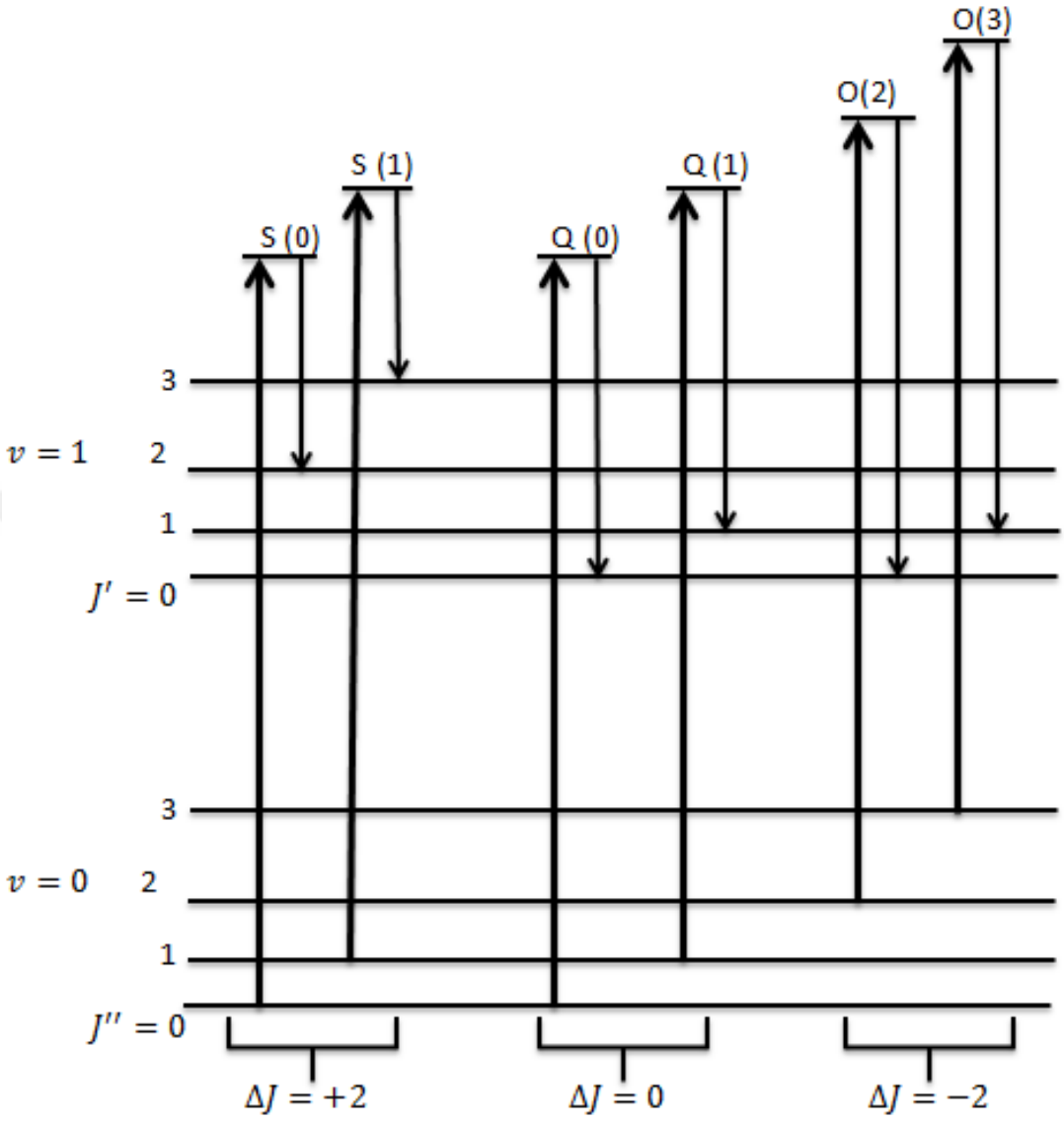

Figure (15) Vibrational Raman Stokes transition

In the case of stoke, the transition will be coming from a low energy vibration state to a high energy vibration state . However, In the case of anti-stokes, the transition will be coming from a high energy vibration state to a low energy vibration state only the conservation of energy. The energy lost by the molecule in this process is gained by the scattering photon again we must consider the $\Delta J = 0, \pm 2$ selection rules. The Figure (16) illustrated [15].

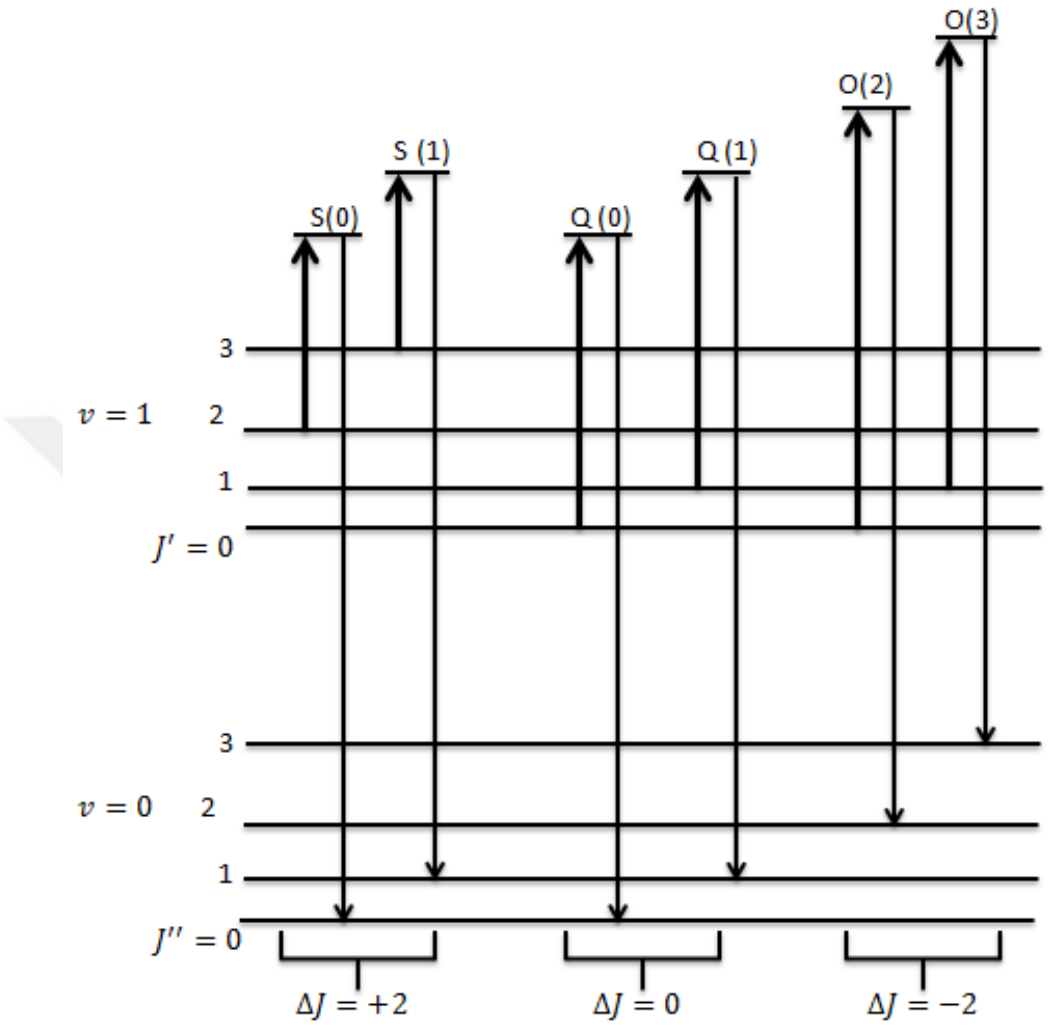

Figure (16) Vibrational Raman anti-Stokes transition

Summary of the above, If the collision is elastic the energy of the photon, as well as the energy of the molecule, will don't change after a collision (Rayleigh) an example of this behavior, what we see in nature, watch the sky blue. The energy difference between the inelastic scattering photon and the incident photon it is exactly the difference between the two energy levels of molecule vibration Δv. If the vibration energy of the molecule is increased after the collision the energy of the scattering

photon is decreased by the same amount and therefore can we detect a long wavelength (Raman stokes). But If the vibration energy of the molecule is decreased after the collision the energy of scattering photon is increase shows the same amount and therefore can we detect short wavelength (Raman anti-stokes) [16].

CHAPTER FOUR

EXPERIMENTAL SECTION AND DATA COLLECTION FOR THE SAMPLE

4.1 Inroduction

Raman Spectroscopy it's a freaked method and used widely to show properties of a sample [6]. When the beam of light or laser is an incident of molecule the most about 99.9999999% of this light will be scattering pass through the sample or molecule with the same frequency, but only a small part, relatively of light will scatter in another way which approximately 0.0000001% will be scattered in different frequency that small value was useful to achieve the requirement of the Raman applications Figure (17) illustrated.

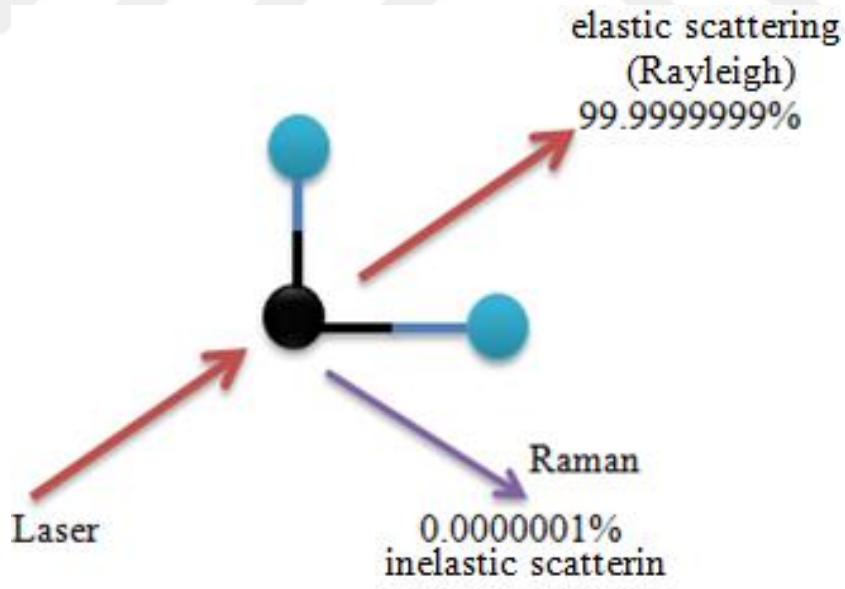

Figure (17) illustrates the ratios of scattering of light through the sample

The incidents of monochromatic green laser (532 nm) on a sample of one layer of graphite (graphene) lead to change on the phonon energy that yielded to emersion two peaks clearly G at 1586 cm^{-1} and 2D at 2691 cm^{-1} which represent the second-rate of D [9]. This observation can be found it by utilizing Raman applications [9, 14]. Investigation of the peaks by the utilization of Raman applications provides data about the structure of the sample and about a number of its intriguing physical characteristics, and from the variation and the deviation between the incident energy of light and the scattering energy of light. We will get on the "Raman Spectra" add to that, we can identify the structure, nature of the discovered materials in recent from knowledge the frequency of the phonon [16]. Figure (18) illustrated.

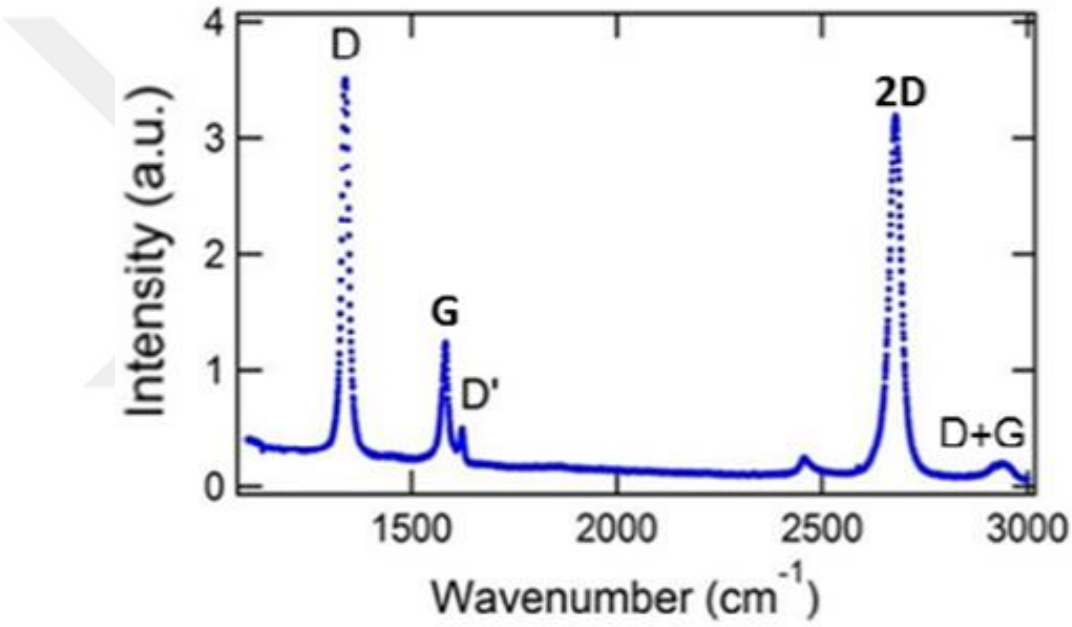

Figure (18) Raman spectrum for a sample of graphene [9]

The two peaks (2D, G) location changes depending on the incident laser energy and the other peaks cannot appear like the peak (D at 1350 cm^{-1}) in the case of the pure graphene, the reason attributed to the crystally symmetry. We can know the numbers of graphene layers from the relation I_{2D}/I_G besides the location and form the peaks where I_{2D}, I_G are representing a peak intensities of 2D and G respectively, and the graphene disorder level can know from ratio I_D/I_G [9,13,16].

The relationship between the (I_D/I_G) from the side and the (L_D) from another side, where L_D is the average dimension for defect and another, will appear two regimes , the first when L_D < 2.9nm , where observe the relationship between (I_D/I_G) and L_D is direct relationship this regime or region called " nanocrystalline graphite", and subject to the formula (4.1).

$$\frac{I_D}{I_G} = \frac{C_\lambda}{L_D^2} \qquad (4.1)$$

Where λ is the wavelength of Raman excitation. If we assume $\lambda = 514\text{nm}$ then C_λ =102 nm^2. While the second regime when L_D > 2.9nm where we observe wherever the L_D increased the (I_D/I_G) decreases this region called "amorphous" and subject to the formula (4.2).

$$\frac{I_D}{I_G} = D_\lambda \, L_D^2 \qquad (4.2)$$

Where D_λ is constant [10]. The Figure (19) illustrated.

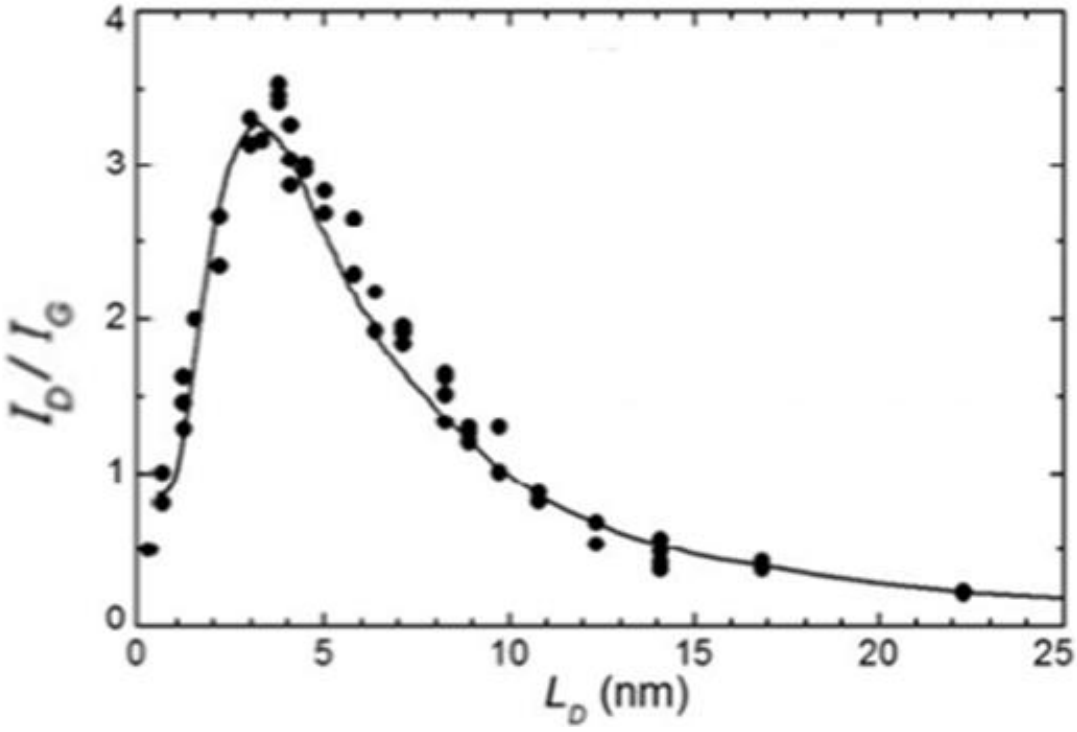

Figure (19) the relationship between (I_D/I_G) related to L_D [9].

Colliding beam of laser which included the incident energy (Ei) and momentum (ki) with the sample and scattered, as a result, a difference going to happen in the energy state (Es) and momentum state (ks) add or we subtract the value of change in the energy and momentum of phonon in the duration of the scattering which is labeled as (Eq) and (q) respectively. To achieve recombine a hole of the incident momentum (ki) with the electron of momentum state (ks), with condition (wave vector q=0).

$Es = Ei \pm Eq$, $ks = ki \pm q$

That means the phonons at the center point Γ or near that, motivated and activated by Raman process. That all above with respect to first order. However, in the second order case, the condition (q=0) will have more relaxed due to bilateral scattering [16]. The two characteristics, two-dimensional and hexagonal shape of graphene it's been given extra feature, the namely linear relation for dispersion at the corners of Brillouin Zone "BZ" labeled K, K' And also call "Dirac" cone [13, 16]. In case of ($q \neq 0$) and low energy states, the two cases of scattering will appear (inter and intra valley) where scattering K→K' or vice versa for the peak D or K→K or vice versa for peak D' Respectively [16].

The hexagonal form of sample graphene gave it arrangement a distinctive of two forms, armchair rim and zigzag rim. Whereas armchair rim only has the ability to show the D peak by the elastic scatter of charge carriers. According to the reference [9] if the polarized of excitation source (laser) was in parallel with the line direction of armchair rim the D peak will get a further strong near that. Unlike in the case of the zigzag rim effect of which would be very simple compared with the previous case.

Also, the developed theories and studies enhanced by the experiments of the process shown that the lonely optical phonon which has behavior longitudinal it has high – effect close to the armchair rim. And the behavior of optical phonon was transverse close to the zigzag rim, therefore the I_G is boosted in the case of the parallel of the polarized excitation source with line direction of an armchair and orthogonal with line direction of the zigzag rim [9]. The Figure (20) illustrated.

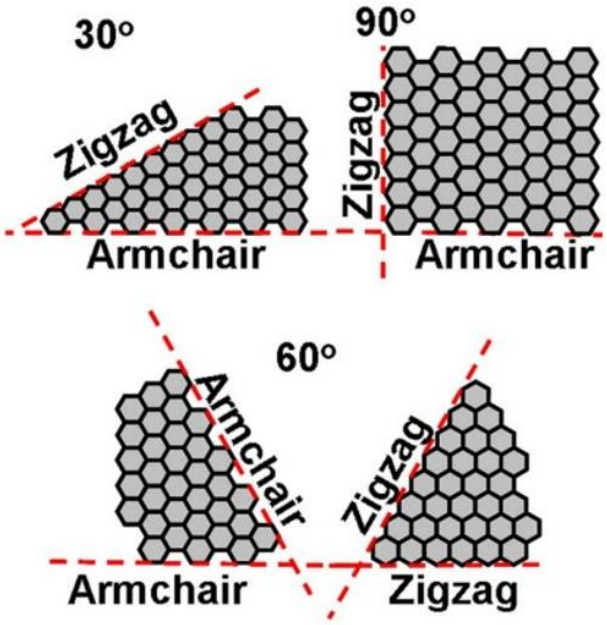

Figure (20) Zigzag and Armchair forms of graphene sample [9]

4.2 Experimental section

4.2.1 Sample preparation

The sample of MWCNTs that which used in the experiment, it was received from Nanografi Co. Ltd. (Turkey) as gift to support of students. In this experiment, my work was done on the NGNC7000 series with carbon purity (90%). The experiment was carried out in the laboratories at Hacettepe University.

4.2.2 Type and specification of the Raman spectrometer

The spectrometer device that utilized in this experiment was one of the device that is produced and have trademarked by DeltaNu Figure (21) illustrated. Where several series wavelengths can be used in this series type of spectrometer such as (532nm,633nm, and 785nm) and used NuSpec Software Figure (22) illustrated. The power of used laser in this device has five choices (low, low-medium, medium, medium-high, high).

We choose three values of Laser Energy which are low, medium and high, 200mW, 100mW, 50mW respectively and the experiment was carried out on those energy parameters. The figure (23) illustrated all the parts of this device.

Figure (21) picture of the Raman spectrometer device

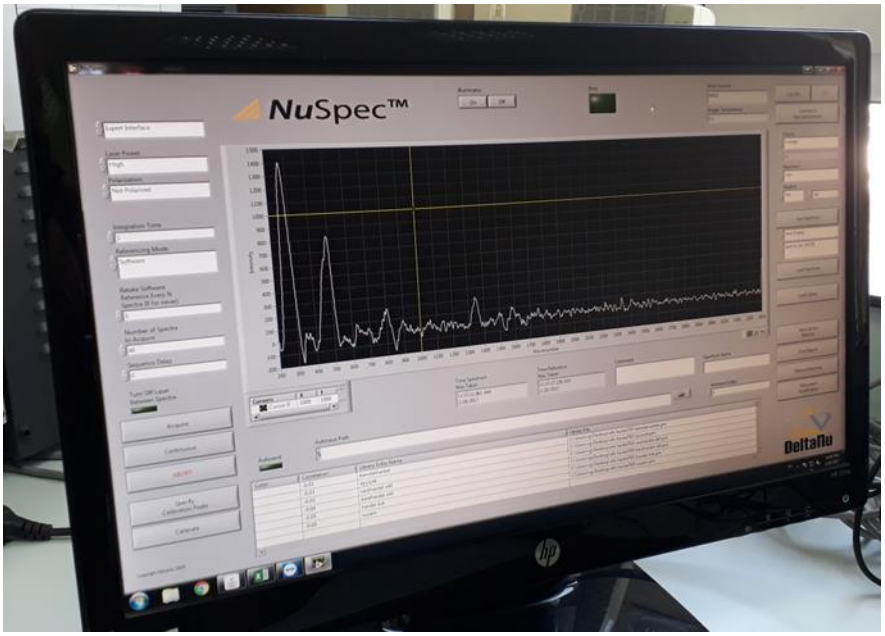

Figure (22) picture of the display screen of the Raman spectrometer device

Figure (23) picture of the parts Raman spectrometer device

4.2.3 Steps and results of the experiment

The first step is taken the sample and place it in the vial and then placed in the sample holder. We have selected the value of the power laser on low power, we followed this step, according to the user manual of the device, so as not to damage the sample. This procedure in general is for all materials samples to protect the samples from damage, while in the case of carbon compounds, we can start from the high degrees of laser power because the temperature of carbon melting up to 3700 C°, but we followed the steps in the user manual of the spectrometer device. From this step we get the spectrum at the figure (24). It is worth noting that this process is automatically only that the values to be changed are being calibrated. And I take the sector of wavenumber (1500 cm^{-1} -1800 cm^{-1}) to focus on the G-band.

- By changing the laser power, we get the spectrum at the Figure (25). And if the power laser change to high on the same sample, we get the spectrum at the Figure (26). For some analysis, we combined the previous three figures in one figure as in Figure (27).

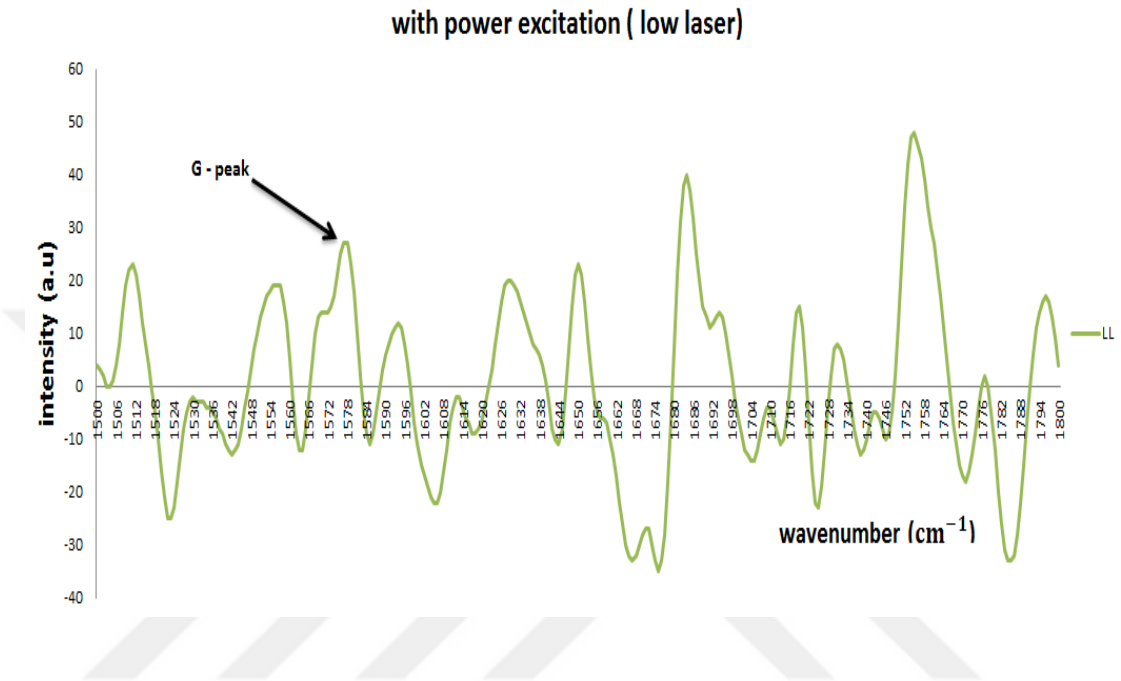

Figure (24) Raman spectrum of sample with low laser 50mW .

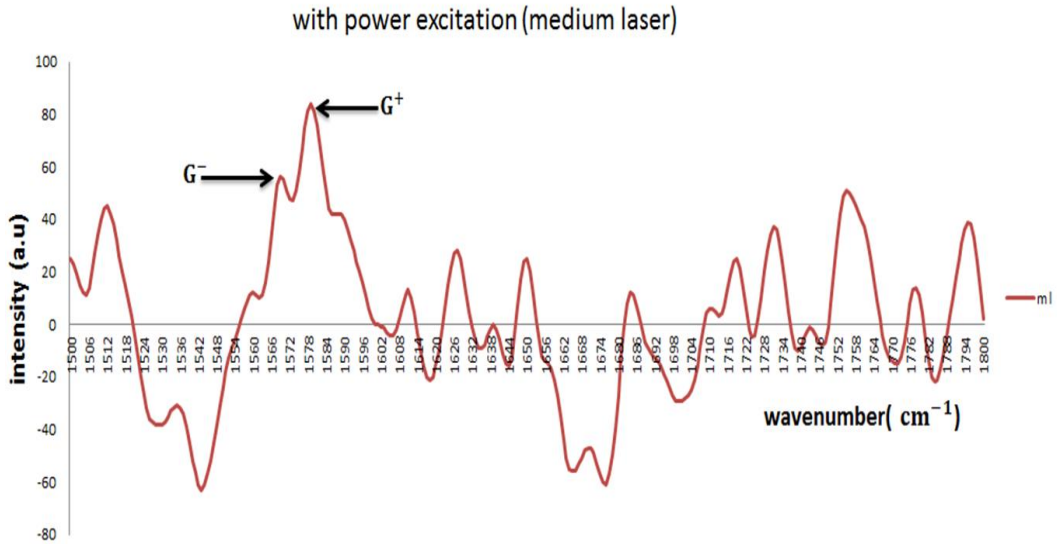

Figure (25) Raman spectrum of sample with medium laser 100mW.

In Figure (25) we observe clearly the ($\mathbf{G}^-$ and $\mathbf{G}^+$), but when the laser power covert of high laser power the form ($\mathbf{G}^-$) will fade away smoothly and it disappears as shown in Figure (26). Whereas the ($\mathbf{G}^-$) would be more flexible with the smaller diameter for the CNTs. In contrast, the ($\mathbf{G}^+$) do not be affected by changes in the diameter of the CNTs.

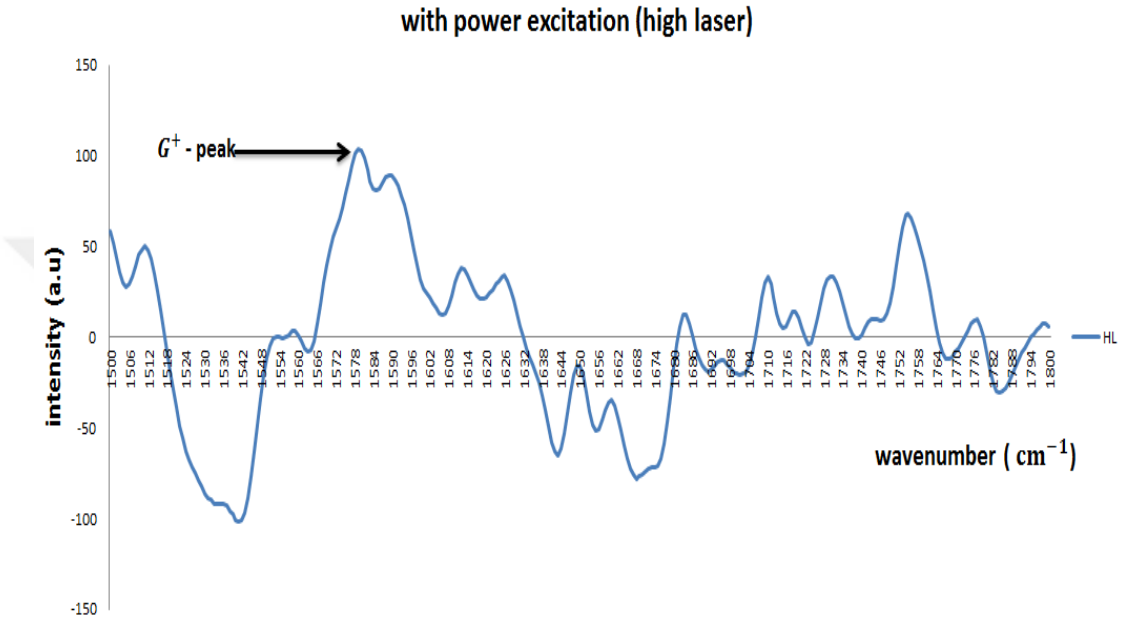

Figure (26) Raman spectrum of sample with high laser 200mW.

In Figures (28,29 and 30) we noticed the stages of the emergence of the D- peak gradually as the laser power increases as in the appearance of the G-peak. This shows that best result we get for the clarity of the spectrum is to be in the case of increased laser power, but to a certain extent and not to the finality otherwise may be a breakdown in the sample.

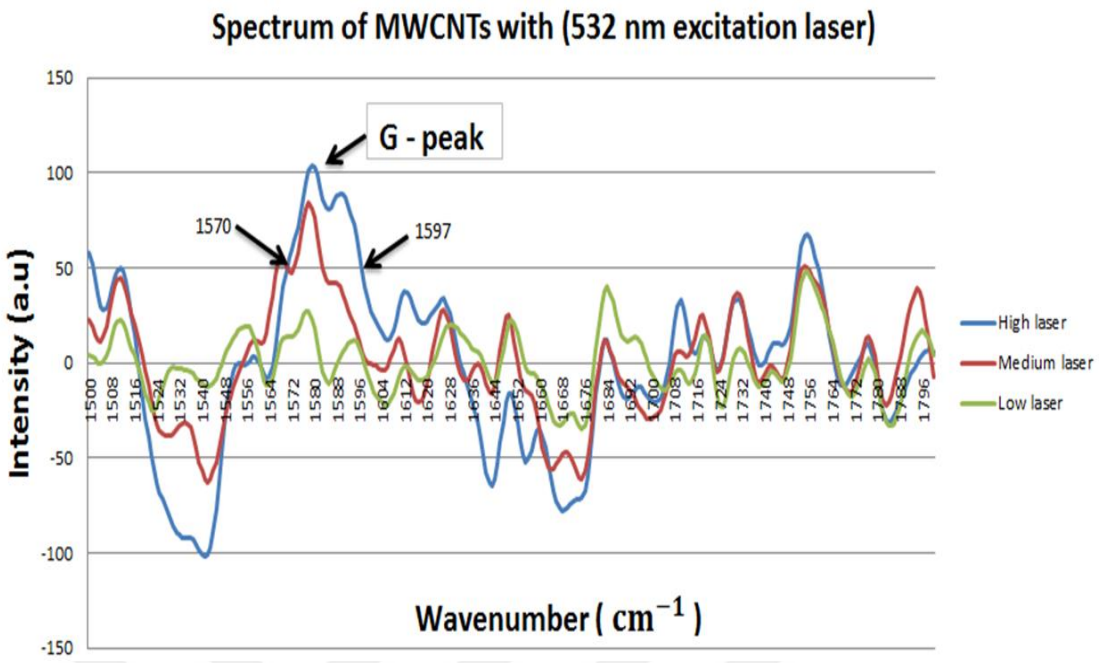

Figure (27) Raman spectrum of sample with combination between the low, medium and high laser cases.

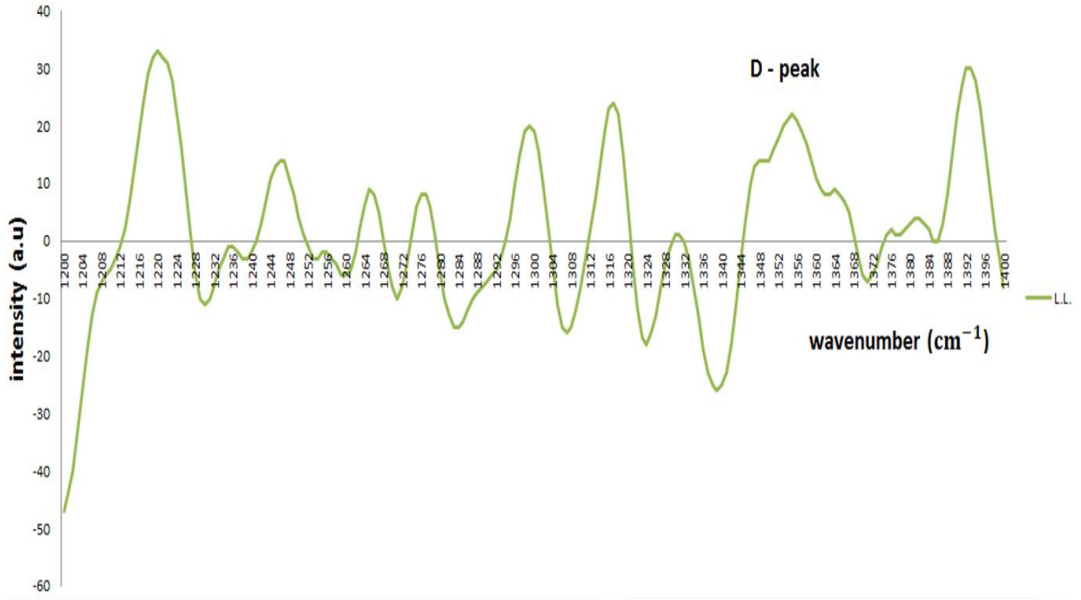

Figure (28) Raman spectrum for MWCNTs show the D - peak with low laser 50mW

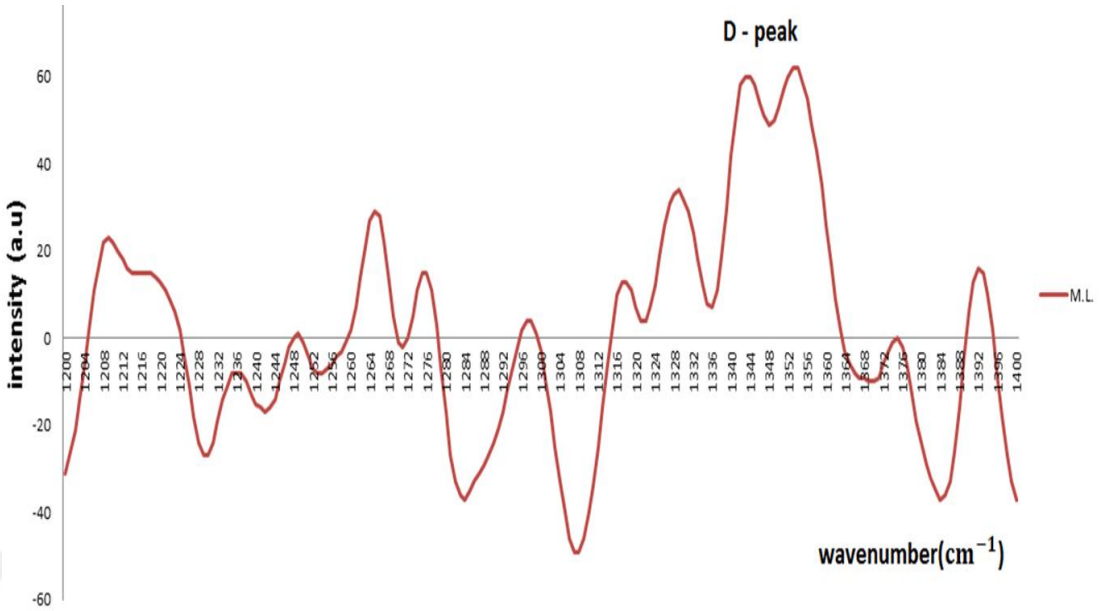

Figure (29) Raman spectrum for MWCNTs show the D - peak with medium laser 100mW

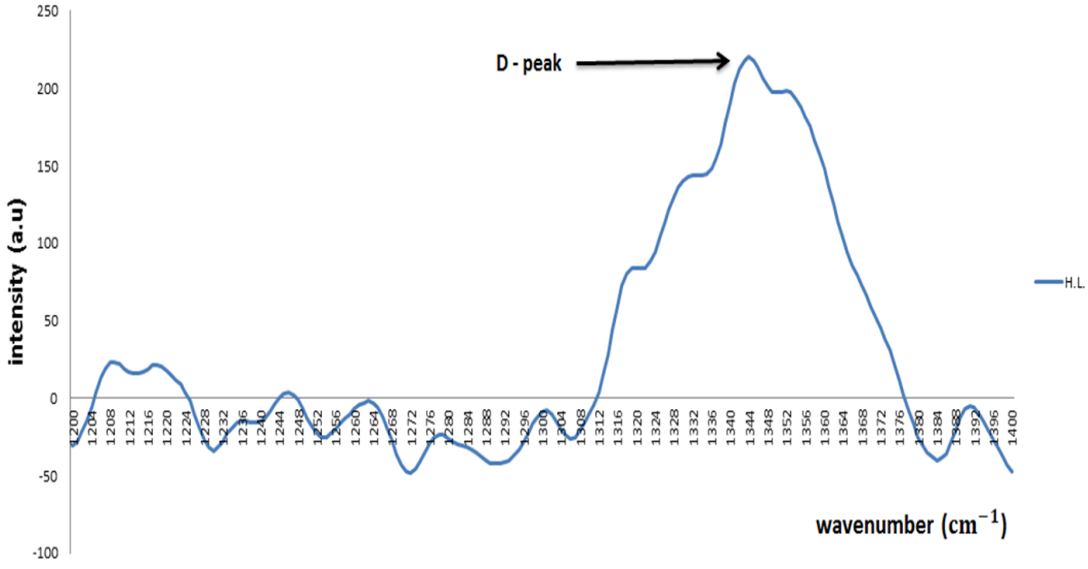

Figure (30) Raman spectrum for MWCNTs show the D - peak with high laser 200mW

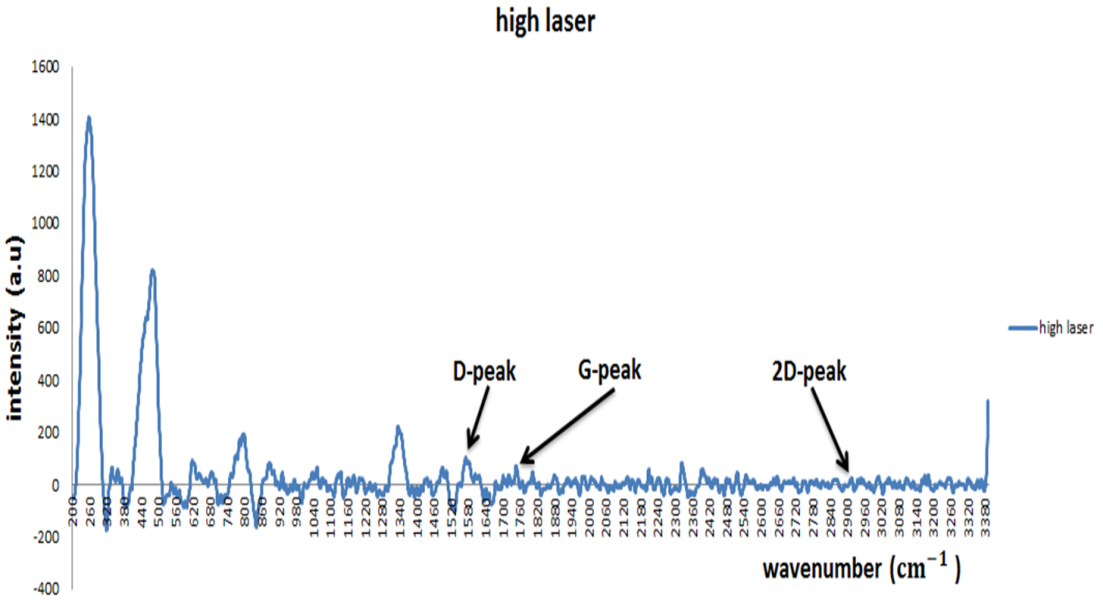

Figure (31) Raman spectrum of sample with full scale of the spectrometer

The Figure (31) represents the spectrum of the sample with full scale of the spectrometer with high power laser, we can be observed the D-peak, G-peak, 2D-peak and the glass peak that appears in the spectrum due to the glass of sample vial as well the Radial Breathing Mode (RBM) which is located less than 600 cm^{-1} [39]. It is important to mention that there is an inverse relationship between the diameter of the CNT and the frequency of RBM in addition to that appearance the RBM in spectrum proof that the CNT it's already exists in the sample.

The increased of the outer diameter of the MWCNTs it is losing some the common qualities with SWCNTs, in another meaning, the features which appeared in the spectrum of SWCNTs doesn't appear in the spectrum of MWCNTs. For instance, the feature of RBM related with the inner diameter change of tubes (< 2nm) can be observed if the resonance situation was well established, however, this doesn't always get it. Therefore, the signal of RBM in case of large diameters is very weak can be noticed [40].

If we focus our attention to Figure (26), we note that with the increase the power of the laser keeps the peak of G in the same location at (1579 cm^{-1}) But the intensity change and the spectrum are more clarity compared with the spectrum in Figure (24), because of the black color of the sample and the absorption is great in this case, so be

useful, we are lifting the power of laser to overcome this case as well as the bypass background noise. As mentioned above, the high power of the laser leads to damage of some samples, but in the case of MWCNTs requires lifting power to get a clear spectrum. But to a certain extent as we note that the higher the laser power the more the shape of the spectrum goes to breakdown. Also by using FWHM method with the G-band that place between (1570 cm^{-1} -1597 cm^{-1}) we can get on the outer diameter of the MWCNT which is equal 27 nm, Figure (27) illustrated. If it is possible to find the number of layers MWCNT if we knew the inner diameter and the gap between the layers is already known, the number of layers can simply be calculated. Or by scanning of the cross section of MWCNTs by using SEM to know the outer and inner diameter and the numbers of layers.

From Figure (27) we can observe the shifted in the spectrum when the power of the laser is increased. And to be more clear, the shifting was explained by the Figure (32) which clarify the shifted in both case medium power laser and low power laser. And Figure (33) explain the shifted between high power laser and low power laser. This shift indicates the sensitivity of the sample to the temperature change resulting from higher laser power, this sensitivity is high, because the color of carbon compounds are black and this helps to absorb energy and also this factor assists the high temperature of the sample compared with light color samples.

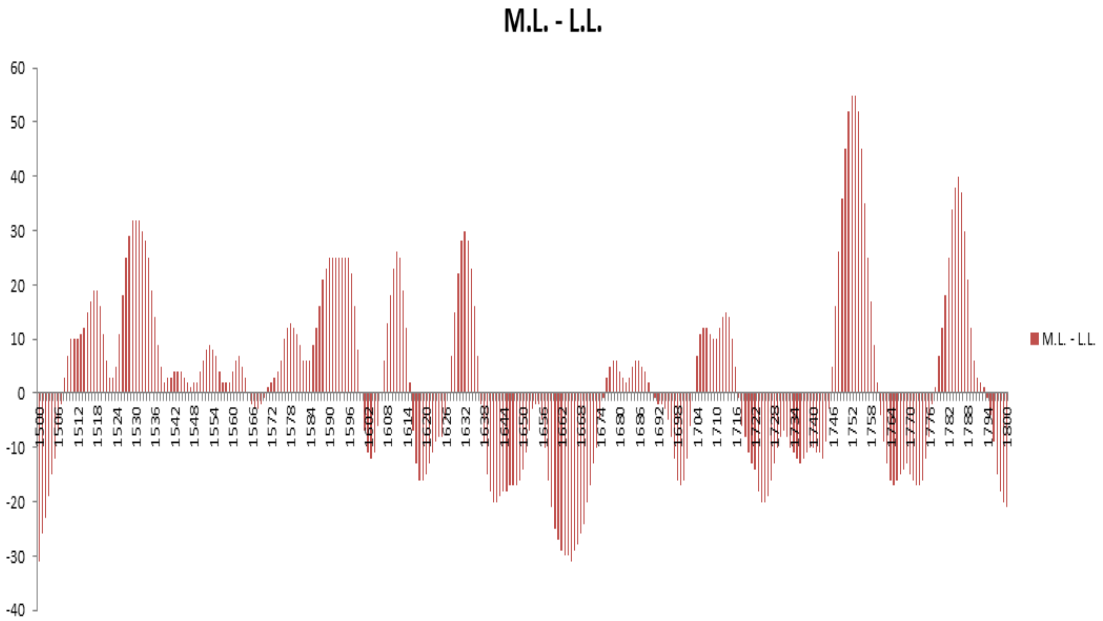

Figure (32) The column chart for the amount of shifting in the spectrum for the medium laser and low laser.

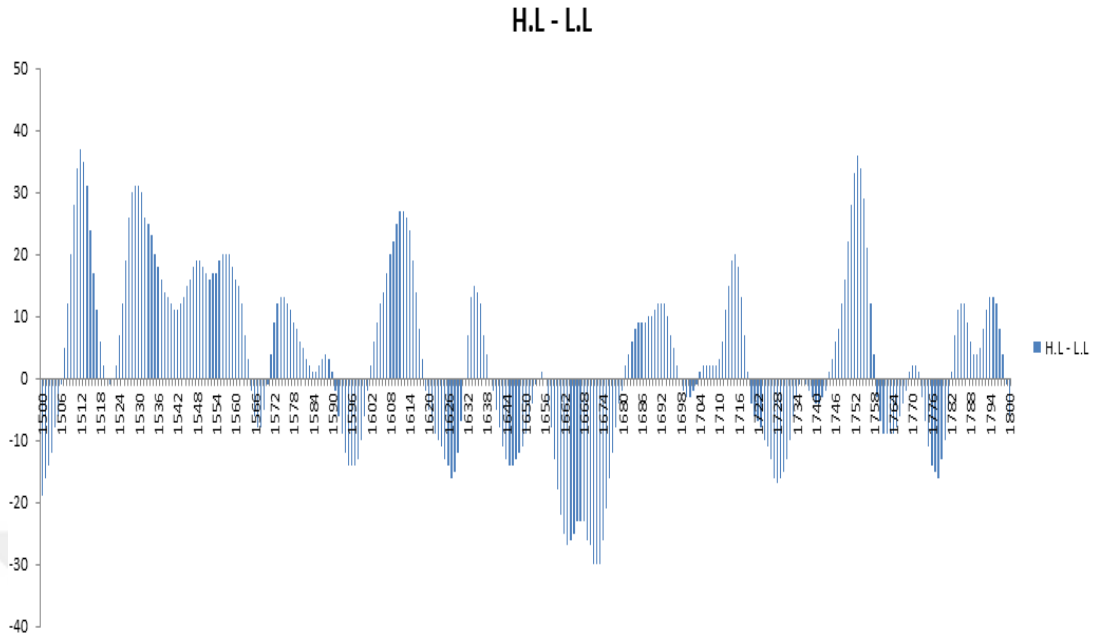

Figure (33) The column chart for the amount of shifting in the spectrum for the high laser and low laser.

CHAPTER FIVE

CONCLUSION

The discovery carbon based optoelectronic materials SWCNTs, MWCNTs and Graphene is the latest revolution in the electronics field. This gave us a strong motivation to study these compounds and conduct some experiments on a sample of MWCNTs. Where some concepts derived and the results of the sample where it was measured the diameter of MWCNT from the spectrum of a sample and the diameter size affects inversely on the signal (RBM). In addition to that, we were able to observe the effect of changing the laser power on the appearance of the peaks in the spectrum compared to the fingerprint of the sample. Where we noticed the change in power of laser starting from low power, the peaks are not appearing clearly, the black color of the sample causes to absorb the amount of power. But, when the power is increased gradually, we can notice the peaks. Signal to noise ratios (S/N) have been taken to overcome noise effects. Also, we were able to observe the tolerance of the sample of the high power of the laser, which in turns raises the temperature of the sample to high degrees with a slight but noticeable impact, that may damage and burn in the case of high temperature. These conclusions gave us motivation to plan for further research and study to develop small electronic components that are built from carbon-derived materials and using in new applications.

REFERENCES

[1**]** Introductory Raman Spectroscopy – Nakamoto – Elsevier

[2**]** Schrader, B. Infrared and Raman Spectroscopy; Schrader, B. ed., VCH Publishers Inc.: New York, 1995; Chapter 1

[3] Theory of Graphene Raman Spectroscopy; Eric J. Heller, Yuan Yang, Lucas Kocia, Wei Chen, Shiang Fang, Mario Borunda, Efthimios Kaxiras

[4] "Optoelectronic with Carbon Nanotubes" by Megumi Kinoshita.

[5] "Raman Spectroscopy in graphene" by L. M. Malard, M. A. Pimenta, G. Dresselhaus, M. S. Dresselhus.

[6] Scientific Background on the Nobel Prize in Physics 2010 (GRAPHENE) compiled by the Class for Physics of the Royal Swedish Academy of Sciences.

[7] "Graphene Synthesis and Applications" Edited by Wonbong Choi, Jo-won Lee

[8] A. K. Geim & K. S. Novoselov. "The rise of graphene" Nature Materials, Vol 6 183-191 (March 2007)

[9] "Raman Spectroscopy of Graphene and Related Materials" by Isaac Childees et al.

[10] Control and Characterization of Individual Grains and Grain Boundaries in Graphene Grown by Chemical Vapor Deposition

[11] A series of lectures "Vibrational Spectroscopy" by Adrian Lee, Feb 2014.

[12] "Modern spectroscopy" fourth edition by J. MICHAEL HOLLAS.

[13] A series of lectures "introductory spectroscopy and structure – Raman scattering" by W. S. Hopkins, Oct, 2014.

[14] "Raman spectroscopy of graphene and graphite: Disorder, electron-phonon coupling, doping and nonadiabatic effects" by Andrea C. Ferrari.

[15] Graphene: A Rising Star on the Horizon of Materials Science. By Ujjal Kumar Sur.2012.

[16] "Raman spectroscopy of graphene and carbon nanotubes" by R. Saito, M. Hofmann, G. Dresselhaus, A. Jorio & M. S. Dresselhaus.2011.

[17] "Graphene: Status and Prospects" by A.K.Geim ,2009 VOL 324 SCIENCE.

[18] " Raman spectrum of graphene with its versatile future perspectives" by S.S. Nanda et al./Trends in Analytical Chemistry 80 (2016) 125–131.

[19] “Graphene: a two type charge carrier system” (Master Thesis) by Magdalena Wojtaszek.2009.
[20] “Raman spectroscopy as a versatile tool for studying the properties of graphene” by Andrea C. Ferrari and Denis M. Basko, VOL 8 APRIL 2013.
[21] “Graphene and Two-Dimensional Materials for Optoelectronic Applications” by Andreas Bablich et al, Electronics 2016, 5, 13; doi:10.3390/electronics5010013.
[22] “Graphene photonics and optoelectronics” by F. Bonaccorso *et al*, VOL 4 | SEPTEMBER 2010.
[23] “graphene transistors” by Frank Schwierz VOL 5 | JULY 2010, doi: 10.1038/nnano.2010.89
[24] “The Prospective Two-Dimensional Graphene Nanosheets: Preparation, Functionalization, and Applications” by Zhi Yang *et al*, Nano-Micro Lett. 4 (1), 1-9 (2012).
[25] “Generation of valley-polarized electron beam in bilayer graphene” by Changsoo Park. JOURNAL OF APPLIED PHYSICS 118, 244301 (2015).
[26] “Raman and Conductivity Analysis of Graphene for Biomedical Applications” by Chao Qiu *et al*, Materials 2016, 9, 897; doi:10.3390/ma9110897.
[27] “Growth of large-area graphene films from metal-carbon melts” by Shaahin Amini *et al*, JOURNAL OF APPLIED PHYSICS 108, 094321 2010.
[28] “Nanographene production from platelet carbon nanofiber by supercritical fluid exfoliation” by Takaaki Tomai, Yuji Kawaguchi, and Itaru Honma. APPLIED PHYSICS LETTERS 100, 233110 (2012).
[29] “Raman fingerprint of charged impurities in graphene” by C. Casiraghi *et al*, APPLIED PHYSICS LETTERS 91, 233108 2007.
[30] “Damage and strain in single-layer graphene induced by very-low-energy electron-beam irradiation” by Katsuhisa Murakami, Takuya Kadowaki, and Jun-ichi Fujita, APPLIED PHYSICS LETTERS 102, 043111 (2013).
[31] “Hydrophilic behavior of graphene and graphene-based materials” by Sebastián R. Accordino *et al*, THE JOURNAL OF CHEMICAL PHYSICS143, 154704 (2015).
[32] “Laser induced non-thermal deposition of ultrathin graphite” by M. Reininghaus et al, APPLIED PHYSICS LETTERS 100, 151606 (2012).
[33] “Temperature dependent Raman spectroscopy of chemically derived graphene” by Matthew J. Allen *et al*, APPLIED PHYSICS LETTERS 93, 193119 2008.

[34] “Carbon nanotubes–properties and applications: a review” by Khalid Saeed and Ibrahim, Carbon Letters Vol. 14, No. 3, 131-144 (2013).
[35] “Carbon Nanotubes and Graphene for Soft Electronics” by Young Hee LEE, Sungkyunkwan University, Korea.
[36] “Nanostructures: a platform for brain repair and augmentation” by Vidu *et al*. June 2014 | Volume 8 | Article 91 |.
[37] “Carbon nanotubes: properties and application” by Valentin N. Popov/Materials Science and Engineering R 43 (2004) 61–102.
[38] “Carbon Nanotubes 101 – Production Methods”
[39] “Evaluating the characteristics of multiwall carbon nanotubes” by John H. Lehman *et. al*, CARBON 49 (2011) 2581 – 2602.
[40] “Characterization of carbon nanotubes by Raman spectroscopy” by S. COSTA *et al* , Materials Science-Poland, Vol. 26, No. 2, 2008.